

ÉCOLE CENTRALE DE NANTES

MASTER CORO-IMARO
“CONTROL AND ROBOTICS”

2020 / 2021

Master’s Thesis

Presented by

Josep Rueda Collell

01/02/2021

Simulation and implementation of a muscular based controllers to assist gait using a hip flexion-extension hip orthosis

Jury

Evaluators: Olivier Kermorgant
Ali Reza Manzoori Associate Professor (École Centrale Nantes)
BIOROB Researcher (EPFL)

Supervisors: Yannick Aoustin
Maura Casadio
Auke Jan Ijspeert
Mohamed Bouri
Andrea Di Russo Professor (Université de Nantes)
Associate Professor (Università di Genova)
Head of the BIOROB (EPFL)
BIOROB Researcher (EPFL)
BIOROB Researcher (EPFL)

Laboratory: Biorobotics Laboratory BIOROB / EPFL

Abstract

In this Master's Thesis we present the methodology followed to obtain a control strategy, based on using torque trajectories, to actuate a motorized hip orthosis with the objective of aiding elderly people in walking, or any kind of people with low muscle power at the hip joint. To obtain these torque trajectories, a novel method based on using neuro-mechanical simulations of human locomotion with reflex-based controllers will be employed. Using a simulator we obtained the torque profile that the virtual human muscles would exert over the hip joint of our neuro-mechanical model based on reflex controllers. With it, we were able to compare the difference between applying a torque profile obtained from measuring the human body and using a verified torque profile obtained from another research work. This thesis will also show the different methodologies and their results used in reconstructing a proper torque profile to actuate the motors, modeling its shape into mathematical functions, and we will include the different methods to detect the beginning and ending of the gait cycle. This will be explained in detail to show the different options taken into account in order to achieve better simulations, some methods for avoiding the problems that have occurred, and some in-depth definitions to properly define good goal functions for our particular optimizer. Our research work also includes tests with the orthosis robot on human subjects in order to seek validation for the final obtained control strategies. We have seen that the profiles found appear to have different outcomes. Both provide assistance, but they contribute with very different levels of comfort for the subject. This Master's Thesis contributes by showing the advantages and disadvantages of using the different methods to extract and model into a mathematical function a torque from a simulation using a neuro-mechanical model based on reflex-based controllers. It introduces expressions to be used as goal functions for a gait optimizer and shows the results of implementing the torque finally found into a real orthosis robot and testing it on real humans. The last of the two found torque profiles has turned out to be very promising and the users reported that the level of assistance was correct as well as the level of comfort.

Acknowledgements

The following thesis work has been carried out at École Polytechnique Fédérale de Lausanne, in the BIOROB department.

I first would like to acknowledge my Master's Thesis supervisors, Dr. Mohamed Bouri, Dr. Maura Casadio and Dr. Yannick Aoustin, for taking me under their wings and guiding me during the Master's Thesis process. Mohamed Bouri accepted me as a collaborating student in the Biorobotics Laboratory (BioRob) of EPFL. I would like to thank him for having given me the opportunity to work on this fascinating project and for all the help provided during all my internship. He has also been very supportive and kind to me, making my experience at EPFL especially fulfilling. Merci beaucoup, Mohamed. A special thanks to Maura Casadio, who has guided me from the very beginning of my thesis, with long meetings and intense discussions, which profoundly influenced my vision and improved not only the project but also my knowledge of the field.

Finally, I would like to show my gratitude to Yannick Aoustin, for assisting me during the thesis. His vast knowledge of the field proved to be of invaluable use at many stages of my project, and he also assisted me with all the never ending paperwork. Thank you again for that.

Working at the Biorobotics Laboratory was a terrific experience. The lab members were very friendly and supportive, and I would like to mention them by name: Zeynep Özge, Jacob Hernandez, Evgenia Roussinova, Amalric Ortlieb, Runfeng Miao, Dawood Ahmed, Annette Carolin, Sébastien Briot, Eugénie Demeure and Seifeddine Ben Khelil. They made my period in Switzerland one of the most remarkable of my life. I would also like to express my gratitude to the BIOROB Department Leader, Dr. Auke Jan Ijspeert, who was helpful and attentive scheduling regular meetings with me to check on my progress regarding my project.

I would like to profess special gratitude to Andrea Di Russo and Dr. Dimitar Stanev, who provided me with all the knowledge needed at the start of the project and followed me during the whole process with weekly meetings, helping me out with all the problems and questions that emerged in my daily progression.

I also would like to thank the jury members: Dr. Olivier Kermorgant and Ali Reza Manzoori for the time and dedication invested in my evaluation.

Abbreviations

ADL	Activity of Daily Living
CNS	Central Nervous System
CPG	Central Pattern Generator
DoF	Degrees of Freedom
EMG	Electromyography
FSR	Force Sensing Resistor
HiBSO	Hip Ball-Screw Orthosis
PLA	Polylactic Acid
RHS	Right Heel Strike

List of Figures

1.1	Illustration of the planes and axes used to reference the human body Source: Adapted from Poluyi, T. (2014). Control System Development for Six Degree of Freedom Spine Simulator. August 2014. [11].	14
1.2	Figure illustrating the gait phases, where: HS is "heel strike", FF is "flat foot", MS is "mid-stance", HL is "heel lift" and TO is "toe off" for the stance phase and where AM is "acceleration to mid-swing" and MD is "mid-swing and deceleration" for the swing phase. Source: Adapted from (2021) www.footbionics.com/Patients/The+Gait+Cycle.html	16
1.3	Representation of the three main leg motions, expressed in the hip joint. Source: Adapted from Mihcin, S., Ciklacakdir, S., Kocak, M., Tosun, A. (2021). Wearable motion capture system evaluation for biomechanical studies for hip joints. Journal of Biomechanical Engineering, 143(4) [14].	17
1.4	The curves illustrate the statistical joint position trajectories of one healthy subject where the black lines represent the mean profiles for the subject and the grey areas represent the mean ± 1 standard deviation. Source: Mills, P. M., Morrison, S., Lloyd, D. G., Barrett, R. S. (2007). Repeatability of 3D gait kinematics obtained from an electromagnetic tracking system during treadmill locomotion. Journal of Biomechanics, 40(7), 1504–1511 [19]. . .	18
1.5	Joint torque trajectories of healthy subjects walking at different speeds. The torques are normalised for the subjects' weight. The vertical line indicates the end of the stance phase of the gait cycle. Source: Schwartz, M. H., Rozumalski, A., Trost, J. P. (2008). The effect of walking speed on the gait of typically developing children. Journal of Biomechanics, 41(8), 1639–1650 [20].	19
1.6	The simplest two-element Hill-muscle model where: The CE is The contractile element of muscle responsible for active force generation. The SEE is the in series elastic element of muscle representing the tendon. Source: Adapted from Miller, R. H. (2018). Hill-Based Muscle Modeling. In Handbook of Human Motion (pp. 1–22). Springer International Publishing[30]. . .	21
1.7	The muscle tendon unit where: the CE is the contractile element of muscle responsible for active force generation. The SEE is the in series elastic element of muscle representing the tendon. The PEE is the parallel elastic element of muscle responsible for the passive force. And α is the angle between the direction of muscle fibers and the direction of the muscle force. Source: AArslan, Y. Z., Karabulut, D., Ortes, F., Popovic, M. B. (2019). Exoskeletons, Exomusculatures, Exosuits: Dynamic Modeling and Simulation. In Biomechatronics (pp. 305–331). Elsevier [34].	22

2.1	Depiction of the eWalk orthosis. 1) emergency stop button, 2) embedded controller enclosure, 3) torso attachment, 4) motors, 5) thigh segments, 6) thigh attachments, 7) foot sensor amplifier boards, 8) instrumented shoes.	23
2.2	Comparison between the actuation systems used by both orthoses	24
3.1	Depiction of the animation of our model in the SCONE Software[40] simulator, after running the healthy gait simulation.	26
3.2	Graph with the values of the hip position and velocity during the whole simulation, where the red lines show the initial values of the position and the velocity, so we can easily see where the same value is repeated.	27
3.3	Biological torque profile that the muscles exert against the hip joint around the lateral axis.	28
3.4	Representation of the activation signals of the hamstring muscles for the right and left legs, where the shaded area is all the range of obtained values, while the solid line is the obtained one once the walking had stabilized. Both legs have the same behaviour. Looking at the graphs it may seem that we only plotted one leg, but in fact, both legs have symmetrical behaviour therefore, the activation signals depict coincident profiles.	28
3.5	Representation of the activation signals of the gluteus maximus muscles for the right and left legs, where the shaded area is all the range of obtained values, while the solid line is the obtained one once the walking had stabilized.	29
3.6	Comparison between the activation signals of the iliopsoas muscles between the motorized and non-motorized legs when using the Alpha torque profile, where the shaded area is all the range of obtained values, while the solid line is the obtained one once the walking had stabilized.	29
3.7	Biological torque profile that the muscles exert against the hip joint around the lateral axis along with its polynomial approximation.	31
3.8	Signal received by the actuators using the polynomial function.	31
3.9	Signal received by the actuators using the polynomial function avoiding the function overshoots.	32
3.10	Signal fitting of the biological torque using Fourier series fitting.	33
3.11	Graphical representation of the fusion between waves of different periods, where the green wave, represents a past wave, the blue wave, represent the current wave, and the red one represent the upcoming one. All of them with possibly different periods.	34
3.12	Example of four waves of different periods being perfectly chained using the mentioned algorithm. Each wave is depicted with a different color. We have no guarantee that the wave will start or end when it should, that is why the four waves seem to start or end at apparently random points. We can also see with a bare eye that some waves are wider, meaning they have a longer period, and on the other hand, if the wave is narrower, its period is shorter.	34
3.13	Comparissons between the shapes of the original torque profile and the resulting torque after the optimization process.	36
3.14	Comparison between the activation signals of the hamstring muscles of the motorized and non-motorized legs when using the optimized biological torque profile, where the shaded area is all the range of obtained values, while the solid line is the obtained one once the walking had stabilized.	36

3.15	Comparison between the activation signals of the gluteus maximus muscles of the motorized and non-motorized legs when using the optimized biological torque profile, where the shaded area is all the range of obtained values, while the solid line is the obtained one once the walking had stabilized.	37
3.16	Comparison between the activation signals of the iliopsoas muscles of the motorized and non-motorized legs when using the optimized biological torque profile, where the shaded area is all the range of obtained values, while the solid line is the obtained one once the walking had stabilized.	37
3.17	Torque profile obtained from [20], and its sinusoidal approximation.	38
4.1	Musculoskeletal model used to simulate in SCONE Software[40], with the names of its muscles.	39
4.2	Evolution of the Geyer model, starting from the bipedal spring-mass model and developing by replacing the springs with muscles controlled by reflex stimulation, where A, B, C, D and E represent the muscles' behaviour during stance phase, while F represents the muscles' behaviour during swing. Source: Adapted from Geyer, H., Herr, H. (2010). A Muscle-reflex model that encodes principles of legged mechanics produces human walking dynamics and muscle activities. IEEE Transactions on Neural Systems and Rehabilitation[41].	40
4.3	Depiction of the SCONE model falling back before implementing the Torso tilt constraint.	43
4.4	Depiction of the SCONE model landing with the toe before implementing the toe-strike constraint.	44
4.5	Block diagram of the proportional control loop used to make the model more robust against drastic changes in the torque	47
4.6	Graph depicting the behaviour of the period for a random case.	48
5.1	Picture of a subject walking on a treadmill while wearing the eWalk orthosis. . .	50
5.2	Block diagram of the proportional control loop used to make the current gain of the torque signal sent to the motors converge to the desired value.	52
5.3	Shape of the Alpha torque profile, obtained using the simulator.	53
5.4	Comparison between the activation signals of the hamstring muscles between the motorized and non-motorized legs when using the Alpha torque profile, where the shaded area is all the range of obtained values, while the solid line is the obtained one once the walking had stabilized.	53
5.5	Comparison between the activation signals of the gluteus maximus muscles between the motorized and non-motorized legs when using the Alpha torque profile, where the shaded area is all the range of obtained values, while the solid line is the obtained one once the walking had stabilized.	54
5.6	Comparison between the activation signals of the iliopsoas muscles between the motorized and non-motorized legs when using the Alpha torque profile, where the shaded area is all the range of obtained values, while the solid line is the obtained one once the walking had stabilized.	54
5.7	Comparison between the theoretical Alpha torque profile and the one received by the actuators, where the solid line is the mean between all the obtained values and the shaded area is the standard deviation.	55
5.8	Comparison between the hip position of the user when no assistance is received and when the Alpha torque profile is being applied on the actuators, where the solid line is the mean between all the obtained values and the shaded area is the standard deviation.	56

5.9	Display of the torque applied to the hip, the hip position and the hip acceleration, where a solid line is the mean between all the obtained values and a shaded area is the standard deviation.	56
5.10	Shape of the Beta torque profile, obtained using the simulator.	58
5.11	Comparison between the activation signals of the hamstring muscles between the motorized and non-motorized legs when using the Beta torque profile, where the shaded area is all the range of obtained values, while the solid line is the obtained one once the walking had stabilized.	58
5.12	Comparison between the activation signals of the gluteus maximus muscles between the motorized and non-motorized legs when using the Beta torque profile, where the shaded area is all the range of obtained values, while the solid line is the obtained one once the walking had stabilized.	59
5.13	Comparison between the activation signals of the iliopsoas muscles between the motorized and non-motorized legs when using the Beta torque profile, where the shaded area is all the range of obtained values, while the solid line is the obtained one once the walking had stabilized.	59
5.14	Comparison between the theoretical Beta torque profile and the one received by the actuators, where the solid line is the mean between all the obtained values and the shaded area is the standard deviation.	60
5.15	Comparison between the hip position of the user when no assistance is received and when the Beta torque profile is being applied on the actuators, where the solid line is the mean between all the obtained values and the shaded area is the standard deviation.	61
5.16	Display of the torque applied to the hip, the hip position and the hip acceleration, where a solid line is the mean between all the obtained values and a shaded area is the standard deviation.	61

List of Tables

- 1.1 Table defining which motions different leg joints can perform and which muscle or muscle group is involved in each motion.

Source: Adapted from (2021) <https://www.physio-pedia.com/Category:Muscles>. 20

Contents

1	Introduction	12
1.1	Motivation	12
1.2	Human locomotion definitions	13
1.2.1	Human gait terminology	13
1.3	Muscular activity and control	19
1.4	Simulation and neuro-mechanical models	20
2	The orthosis	23
2.1	Robot Design	23
2.2	Comparison between eWalk and HiBSO	24
3	Methodology	25
3.1	Applying the biological torques of a healthy gait	25
3.1.1	Healthy gait simulation	25
3.1.2	Mathematical model of the healthy gait	30
3.2	Applying reference torques of a healthy gait	38
4	SCONE Software Simulations and Methodology	39
4.1	The musculoskeletal model	39
4.2	The SCONE optimizer	41
4.3	The SCONE cost functions	41
4.3.1	Go as far as possible	42
4.3.2	Torque minimization	43
4.3.3	Torso tilt	43
4.3.4	Toe-strike	44
4.3.5	Symmetric walking	44
4.3.6	Less consumption for the motorized leg	45
4.4	Simulator approach	47
5	Experiments	49
5.1	Experiment approach	49
5.1.1	Experiment description	49
5.1.2	Experiment details	50
5.2	Alpha experiment	52
5.2.1	Simulation evaluation	52
5.2.2	Experiment Evaluation	55
5.3	Beta experiment	57
5.3.1	Simulation evaluation	57
5.3.2	Experiment evaluation	60

6 Conclusions and Further Work	63
Bibliography	65

CHAPTER 1

Introduction

1.1 Motivation

Mobility is often a central problem for the quality of life of people who have muscle weaknesses. The causes of these weaknesses are diverse but lead to similar inconveniences. Difficulties in walking have consequences on both physical and psychological health. In many cases, they lead to loss of independence and can cause depression[1].

The upcoming half century will see a dramatic aging in population, which will result in a higher proportion of elderly age groups in the populace. The global fraction of the elderly population (aged 65 years or older) will rise from 5 to 14% in the presently poor countries and from 14 to 26% in the rich countries from 2000 to 2050[2]. In consequence, the need for new technologies to assist walking and walking-related activities will become more and more significant.

Deficiencies in walking, though quite common, can stem from very different causes, due to the heterogeneity of this population. But reduced muscular force is one of the most frequent. On the other hand, in terms of actual movement, in theory and in the absence of any pathologies, there are no significant differences between seniors and younger subjects regarding their gait patterns[3].

However, a vast majority of old people have the worst reaction times and have a higher energy consumption when walking[4] and they require more brain resources to recover from an external perturbation[5]. Also, due to their existing medical conditions, most seniors tend to display notable differences in their gait behaviour.

The aim of assistive robotics is the production of exoskeletons that can assist the user in performing a specific range of movements such as walking or carrying loads[6]. Over the last decades, actuated orthotic devices have been used in order to help people suffering from gait disorders, and autonomous devices have even allowed people with spinal cord injuries to walk again by mobilizing their paralyzed limbs [7].

In this thesis, we focus on a case where the wearer is in charge of his/her own movements and the device simply provides assistance to the hip joint using pre-computed torque trajectories.

Walking assistive devices need to work in interaction with their user as intuitively as possible. The person wearing an assistive orthosis should be able to decide which movement to make and when should it be performed. Therefore, the device should be transparent (zero impedance) when the user does not need any assistance and apply forces only when required[8].

As a final objective, the device should be perfectly innocuous, meaning that the pilot could barely feel that he or she is wearing any device, although it would be aiding the user. While the field is largely covered, the number of devices targeting the assistance of the hip flexion-extension to face ageing of the population or similar issues does not exceed five devices based on our knowledge.[\[6\]](#)

Even though the elderly people are in need of assistance, they surely do not want to have movements imposed on them by a robotic device, and therefore, the control strategy presented in this thesis takes into consideration the possibility of the user wanting to change his/her walking speed as he/she desires. Thus, the algorithm should add the right amount of torque only when it is required.

To find the perfect torque trajectory, we have used a model of the human body and with a virtual hip actuator added to it. Using a simulator we have experimented with different methodologies to find a proper torque profile to actuate the motors including the different methods to detect the beginning and ending of the gait cycle.

For the purposes of this master's thesis, exoskeletons and orthoses should be differentiated: Both are defined as "worn" mechanical devices that work in concert with the operator's movements. But in general, the term "exoskeleton" is used to describe a device that augments the performance of an able-bodied wearer, whereas the term "orthosis" is typically used to describe a device that is used to assist a person with a limb pathology[\[9\]](#). Since this research work is focused on helping people with low muscle strength or other kinds of pathologies, from now on, we will refer to the particular device used in this research work as an "orthosis".

1.2 Human locomotion definitions

The bipedal walk is the method humans use for locomotion, and as such it is one of the most important tasks of our Activity of Daily Living (ADL). Other locomotion methods such as running or hopping may be used but walking remains the most natural method. If no injuries are presented, a human can keep his/her balance while performing a motion and while remaining still, but because of the differences in the musculoskeletal structure of each individual, gait differences may be observed, and therefore, every individual optimizes his gait differently according to his own body [\[10\]](#).

1.2.1 Human gait terminology

In this subsection, we will define some important aspects of the human gait and the main muscles involved in the activity of walking.

Definition of the planes and the reference axes

The human body locomotion is usually described using three main planes as references, each one being perpendicular to the others and all of them intersecting the body centre of mass as we can see in Figure [1.1](#):

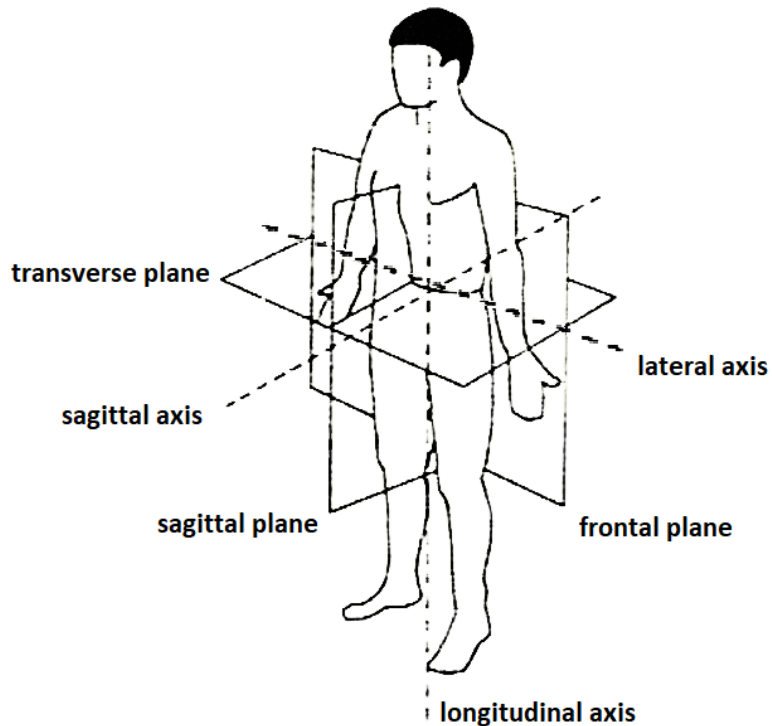


Figure 1.1: Illustration of the planes and axes used to reference the human body

Source: Adapted from Poluyi, T. (2014). Control System Development for Six Degree of Freedom Spine Simulator. August 2014. [11].

- The sagittal plane is the vertical plane that divides the body into the left and right parts.
- The frontal plane is the vertical plane that divides the body into the anterior and posterior parts.
- The transverse plane is the horizontal plane that divides the body into the lower and upper parts.

When we describe a movement of the human body, we usually describe it as a movement that is parallel to one of these planes; for example, walking is considered to be an activity that takes place along the sagittal plane. The intersection of our planes forms three different axes, which may also be used to describe body movements.

- The lateral axis is described by the intersection between the frontal and the transverse planes.
- The sagittal axis is described by the intersection between the sagittal and the transverse planes.
- The longitudinal axis is described by the intersection between the sagittal and the frontal planes.

We must point out that this thesis will stick to the criteria described in this section, but the reader must take into consideration the fact that other scientific research works might refer to these planes and axes with other names.

Definition of stride and step

A stride is defined as a complete walking cycle, or in other words, the combination of one right step and one left step. The convention dictates that the stride starts at the Right Heel Strike (RHS) and each step of each leg starts and ends with a Heel strike (HS). A step can be quantified by measuring the distance between the heel position at the start of the step and its position at the end, both coinciding with a heel-strike. The typical step length for a male adult is $0.8 \pm 0.09\text{m}$ [12], but note that right and left steps might not be necessarily identical on both sides, especially when pathologies are present.

The gait cycle

The gait cycle is the convention used in biomechanics to describe walking. The gait cycle defines the motion of the legs, regarding the behaviour of the feet. When a human walks, the two feet alternatively lift and move forward enabling the displacement of the whole body. Thus, the different positions of the feet dictate the different phases this gait cycle can be split into starting from the heel on the ground, performing a step and finishing with the same heel on the ground for a second time.

In order to clearly define the human biomechanics of the gait cycle, the gait is divided into two phases: the stance phase and the swing phase. The stance phase is defined as the interval in which the foot is on the ground, it covers up to 60% of the gait cycle and it has been subdivided into five stages depending on the contact with the ground: the “heel strike”, “flat foot”, “mid-stance”, “heel lift” and “toe off”. On the other hand, the swing phase is defined as the interval in which the foot is not in contact with the ground and it is also subdivided into two stages: the “acceleration to mid-swing” and the “mid-swing to deceleration”.

The “heel strike” stage starts when the heel lands on the ground and ends when the whole foot is in contact with the ground. The “flat foot” stage is defined as the moment when the whole foot is on the ground but the other leg is still in contact with the ground. Mid-stance is said to be when the whole body is being supported on one foot. The “heel lift” stage begins when the heel begins to leave the ground. The “toe off” stage begins as the toes leave the ground. This stage also represents the start of the swing phase. The “acceleration to mid-swing” stage starts when the foot leaves the ground and both legs cross one another. The “mid-swing to deceleration” stage starts when both legs are aligned, and ends when the foot is in contact with the ground.

This can be better seen in Figure 1.2

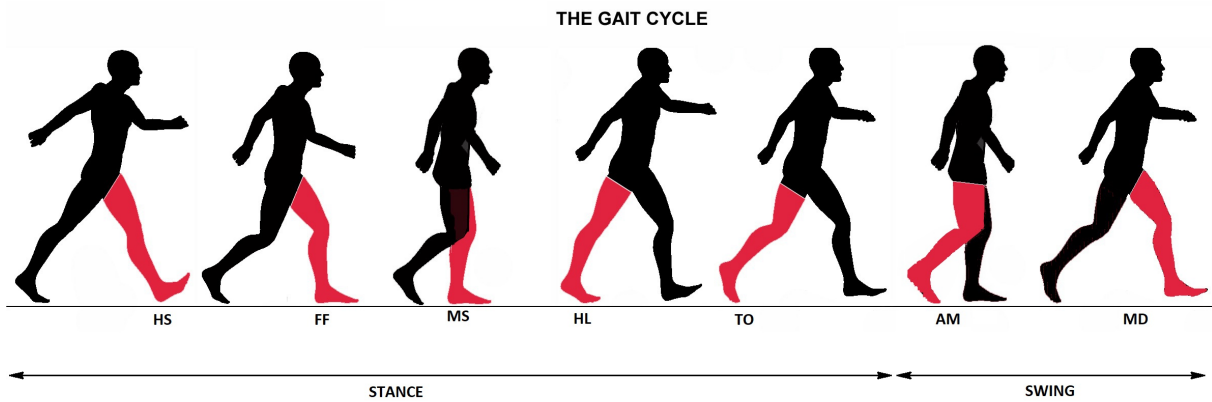


Figure 1.2: Figure illustrating the gait phases, where: HS is "heel strike", FF is "flat foot", MS is "mid-stance", HL is "heel lift" and TO is "toe off" for the stance phase and where AM is "acceleration to mid-swing" and MD is "mid-swing and deceleration" for the swing phase. Source: Adapted from (2021) www.footbionics.com/Patients/The+Gait+Cycle.html

This image highlights left leg heel strike (HS), flat foot (FF), mid-stance (MS), heel lift (HL) and toe off (TO) for the stance phase, and the acceleration to mid-swing (AM) and the mid-swing to deceleration (MD) for the swing phase [13].

Also, another non-mutually exclusive convention that is extensively used is when both feet are in contact with the ground, we might refer to it as "double support" while when only one foot is in contact with the ground we can refer to it as "single support".

Leg motions

The terminology used to describe the different leg motions will be described here:

- Flexion and extension are movements that refer to increasing and decreasing the angle in the sagittal plane and around the lateral axis.
- Adduction and abduction are movements that refer to increasing and decreasing the angle in the frontal plane and around the sagittal axis.
- Internal and external rotations are movements that refer to increasing and decreasing the angle in the transverse plane and around the longitudinal axis.

Figure 1.3 provides a graphical representation of all 3 motions:

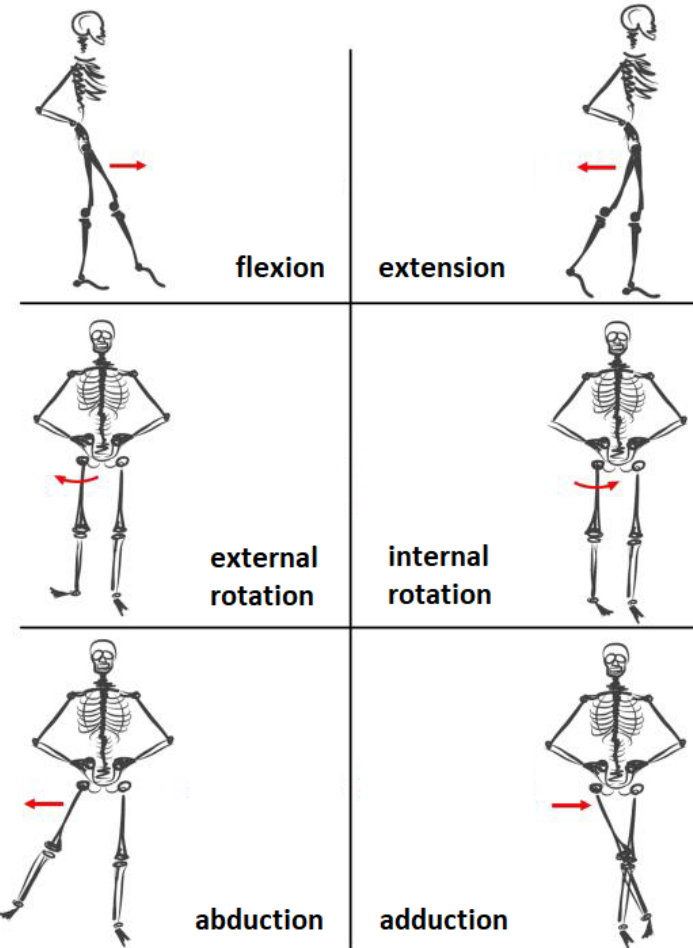


Figure 1.3: Representation of the three main leg motions, expressed in the hip joint.

Source: Adapted from Mihcin, S., Ciklacakdir, S., Kocak, M., Tosun, A. (2021). Wearable motion capture system evaluation for biomechanical studies for hip joints. Journal of Biomechanical Engineering, 143(4) [14].

That being said, according to [15], three main articulations compose the leg bio-mechanical structure:

- The hip is a spherical articulation and as such, it possesses all the three motions previously presented.
- The knee is a 1 Degree of Freedom (DoF) articulation and enables only flexion/extension.
- The ankle has two DoFs. The first one enables internal and external rotations. Although in other scientific research works it might be referred to as a second knee rotation. The second one is the dorsi/plantar flexion, which corresponds to flexion/extension motion. This movement is a combination of several articulations which involve the foot and the ankle, and its axis of rotation is not all parallel to any of the three main axes defined above.

Gait kinematics and dynamics

Each human has a different gait[16], but for each joint, standard trajectories can be identified during walking[17][18]. Figure 1.4 displays these standard intervals according to[19]:

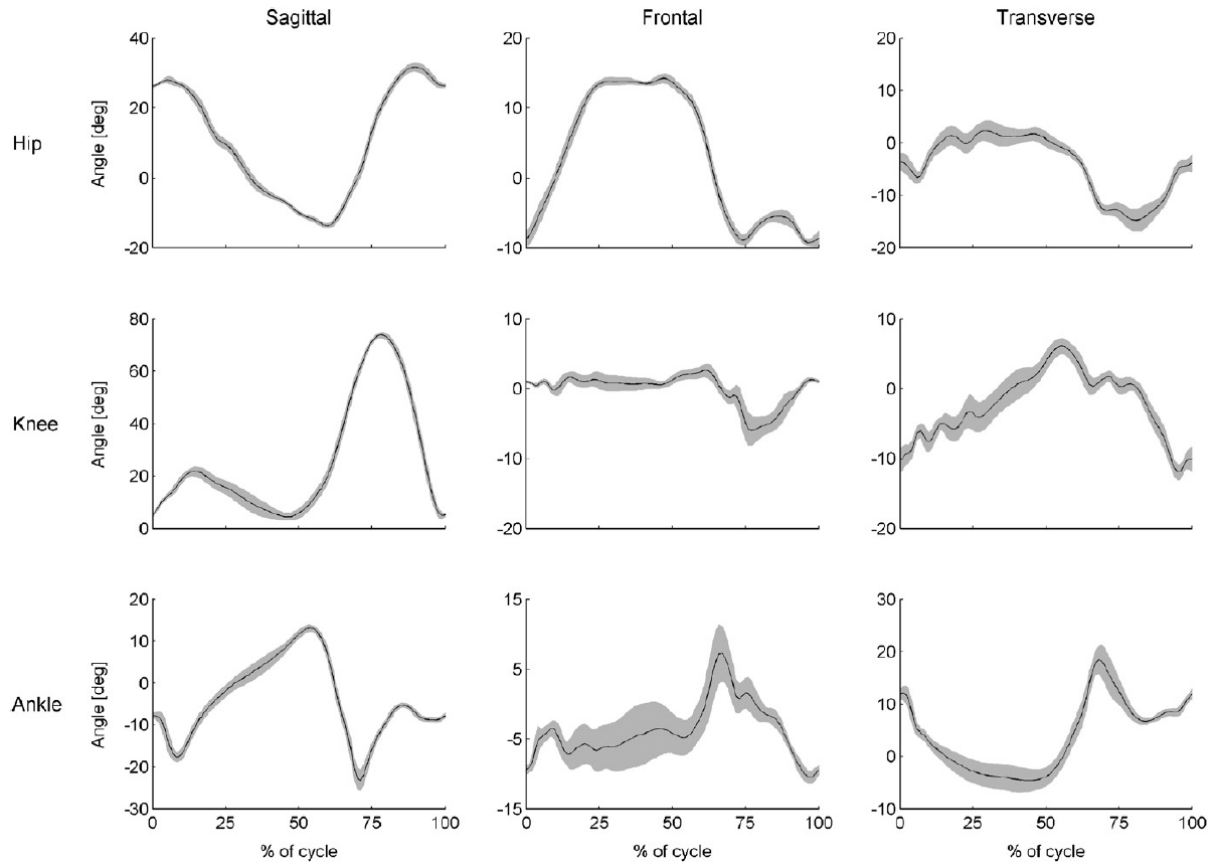


Figure 1.4: The curves illustrate the statistical joint position trajectories of one healthy subject where the black lines represent the mean profiles for the subject and the grey areas represent the mean ± 1 standard deviation.

Source: Mills, P. M., Morrison, S., Lloyd, D. G., Barrett, R. S. (2007). Repeatability of 3D gait kinematics obtained from an electromagnetic tracking system during treadmill locomotion. Journal of Biomechanics, 40(7), 1504–1511 [19].

In order to follow the previously presented kinematic trajectories, the articulations need to receive torques and forces. These torques are presented in Figure 1.5 according to [20] and where we can see that the torque provided relies on the speed of the gait:

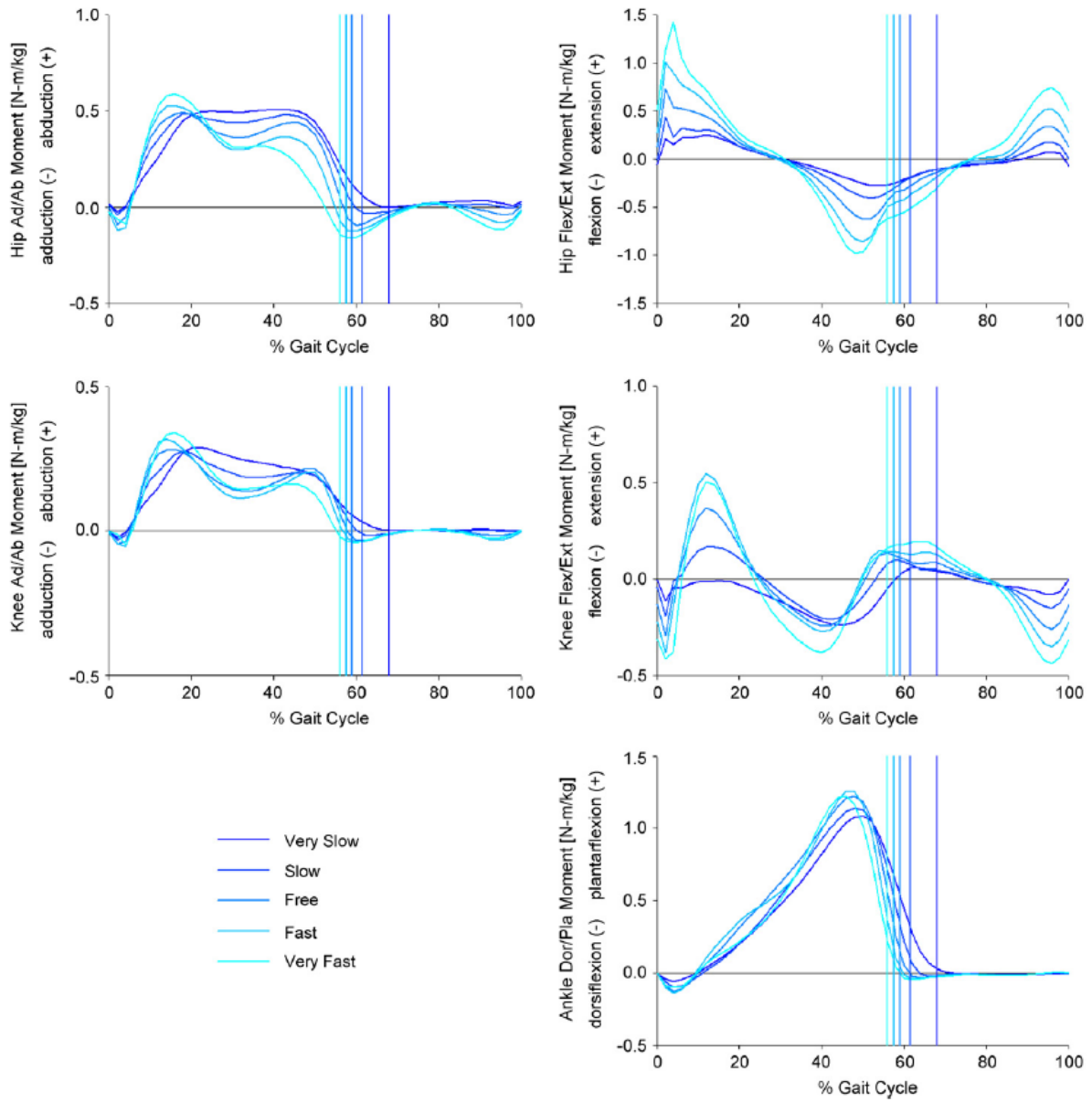


Figure 1.5: Joint torque trajectories of healthy subjects walking at different speeds. The torques are normalised for the subjects' weight. The vertical line indicates the end of the stance phase of the gait cycle.

Source: Schwartz, M. H., Rozumalski, A., Trost, J. P. (2008). The effect of walking speed on the gait of typically developing children. Journal of Biomechanics, 41(8), 1639–1650 [20].

It must be taken into consideration that the definition of speed in the previously mentioned paper is subjective, meaning that the experimentation subject decided how to qualify how fast or slow he/she was walking by using his/her own criteria.

1.3 Muscular activity and control

The torques that human muscles apply at the articulations require the action of several muscles. Since muscles can only produce force when they contract, at least two muscles are required to perform a motion in both directions. One particular phenomenon that we can see in human legs is one muscle being used to perform several motions, for example, the quadriceps have an effect on knee extension but also on hip flexion. A simplified version of the leg muscular

system with only seven muscle groups can be used for describing the walking cycle[21]. Table 1.1 displays which muscle group is needed to perform each leg motion:

Articulation	Motion	Muscle/Muscle Group
Hip	Extension	Gluteus maximus
		Hamstrings
	Flexion	Iliopsoas
		Tensor fasciae latae*
	Abduction	Quadriceps
		Gluteus medius
	Adduction	Gluteus minimus
	Internal rotation	Adductor Magnus
		Tensor fasciae latae
	External rotation	Gluteus medius
		Gluteus minimus
		Triceps coxae
		Obturator externus
		Quadratus femoris
Knee	Extension	Quadriceps femoris
	Flexion	Hamstrings
Ankle	Internal rotation	Popliteus
		Hamstrings
	External rotation	Biceps femoris
	Flexion	Tibialis anterior
	Extension	Triceps surae

*Accessory muscle

Table 1.1: Table defining which motions different leg joints can perform and which muscle or muscle group is involved in each motion.

Source: Adapted from (2021) <https://www.physio-pedia.com/Category:Muscles>.

The coordination and activation of all the muscles had always thought to be managed by the Central Nervous System (CNS), with the basic motor trajectories being initiated at the brain[22]. However, recent studies have stated that the basic motor trajectories are generated at the Central Pattern Generator (CPG) at the spine level[23] where reflexes take a major role in walking since when unexpected perturbations arise, reflexes help to correct the posture, increasing the gait efficiency.

The particular model we will use for our simulations is a neuro-mechanical model based on reflex-based controllers. More detail regarding our specific model can be seen in section 4.1 The musculoskeletal model

1.4 Simulation and neuro-mechanical models

Musculoskeletal simulations can complement experiments in designing assistive devices. They have proven to be very useful when complementing experiments in designing assistive devices. Using simulations to accurately predict the effects of an assistive device is a substantial challenge, as taking into account the device comfort is a very difficult task [24][25]. However, if the model employed is accurate enough, by using a simulator we can explore hypothetical cases through massless devices with frictionless joints, or without power limitations. We can also optimize the devices for a specific objective, such as minimizing muscle activation for a wide

diversity of users with very different physiognomies[26][27][9].

Simulations can also predict how devices might affect the energy consumption of individual muscles, therefore allowing one to take decisions on which joints should be targeted with assisting devices and, on the other hand, one can estimate how real devices would affect the muscle activity [27]. In turn, the results of experimental studies can be used to further validate and improve the predictive capability of simulations [28].

When simulating gait, it is desirable for models based on muscle activation to account for metabolic energy expenditure. A good method for measuring energy consumption in humans, according to [29], is by using thermodynamic principles. These methods have shown to be effective in real experiments, but are hard to implement in simulations and not suitable for optimization of locomotion. Because of that, a majority of the models based on muscle activation are Hill-based i.e. Hill muscle models.

Hill muscle models consist principally of two type of elements: a contractile element (CE) and one or several elastic elements (SE), as you can see in Figure 1.6 (more complex elements can be found, like dampers, but they are not as common):



Figure 1.6: The simplest two-element Hill-muscle model where: The CE is The contractile element of muscle responsible for active force generation. The SEE is the in series elastic element of muscle repre-senting the tendon.

Source: Adapted from Miller, R. H. (2018). Hill-Based Muscle Modeling. In Handbook of Human Motion (pp. 1–22). Springer International Publishing[30].

Due to this simplicity, Hill-based muscle models are the most commonly used actuators in computer neuro-muscular models due to their ease of implementation[31].

The most known and used Hill-muscle model is the Muscle-Tendon Unit[32]. The muscle tendon model, includes a parallel elastic element as van be seen in Figure 1.7. This elements represent The “passive” force of the muscle, which is the force that a muscle exerts due to its own material properties in the absence of activation signal[33].

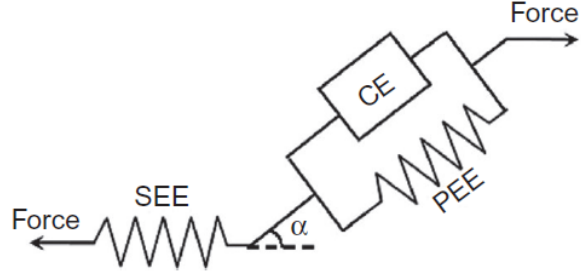


Figure 1.7: The muscle tendon unit where: the CE is the contractile element of muscle responsible for active force generation. The SEE is the in series elastic element of muscle representing the tendon. The PEE is the parallel elastic element of muscle responsible for the passive force. And α is the angle between the direction of muscle fibers and the direction of the muscle force.

Source: AArslan, Y. Z., Karabulut, D., Ortes, F., Popovic, M. B. (2019). Exoskeletons, Exomusculatures, Exosuits: Dynamic Modeling and Simulation. In Biomechatronics (pp. 305–331). Elsevier [34].

Even though these Hill-type muscle models are not based on realistic muscle architecture, the bio-mechanical behavior of a real muscle can be practically simulated with relatively low computational power since only three parameters determine the force production capability of the muscles, name the instantaneous muscle length, the instantaneous muscle velocity and the instantaneous activation level[34]. And even though the Hill-type muscle model provides a practical method for simulating the muscle behaviour, the current drawback of using the Hill-type models is that identifying the model parameters can be a challenging task since it has to be done experimentally[35] and it gets rapidly obsolete due to historical changes in the capability of the muscle to produce force[36].

Skeletal muscles produce force and perform work on the skeleton, at the cost of consuming metabolic energy. And in light of the growing interest in simulations based on Hill-muscle models, there has been considerable interest in adapting Hill-based muscle models such that whole-body energy consumption can be measured during simulations of locomotion [28].

A simple model of muscle energy expenditure was presented in [37], which stated that the metabolic energy consumption of a particular muscle generally depends on its activation and its current kinematic state. Therefore, in several studies the energy consumption is assumed to be proportional to the muscle activation [30]. The activation of a particular muscle is the amount of electric signal that a muscle receives, normally expressed as a percentage in a 0-1 scale, which determines which fraction of the muscle strength it will use.

CHAPTER 2

The orthosis

In this research work we have developed control strategies for eWalk orthosis, provided by the mechatronics company Sonceboz.

The eWalk is an active orthosis designed to assist the hip flexion-extension of the elderly or people with low strength in hip muscles. Thus, it is designed to provide additional torque on the human hip joint around the frontal axis.

2.1 Robot Design

The eWalk orthosis robot starts from the “torso attachment”. This part is attached to the user’s body using two adjustable plastic straps. It is made of 3D-printed Polylactic Acid (PLA) plastic and is padded on the inside to improve comfort.



Figure 2.1: Depiction of the eWalk orthosis. 1) emergency stop button, 2) embedded controller enclosure, 3) torso attachment, 4) motors, 5) thigh segments, 6) thigh attachments, 7) foot sensor amplifier boards, 8) instrumented shoes.

In its back, we can find the embedded controller enclosure, where all the electronic components are connected, including the “instrumented shoes” and the “emergency stop button”. Two motors are screwed to the “torso attachment”, and, using the “thigh segments” which are made of carbon fiber, they connect with the “thigh segments”. These motors provide flexion/extension motion, which corresponds to the only actuated DOF of the robot (per leg). This rotation is made possible by the fact that the hip spherical joint is approximately aligned

with the motor axis around the lateral axis passing through the head of the femur. The “thigh attachments” are also made of 3D-printed PLA plastic and are padded on the inside too. They uses two elastic Velcro straps per leg to attach themselves to the user’s leg.

The electronic design starts with a BeagleBone embedded in the controller enclosure. It includes a Wi-Fi drive, used for debugging and testing purposes. It also includes a Bluetooth drive that handles the communication with a heart-rate sensor, which provided useful data during the experiments.

The sensorized shoes incorporate a set of pressure sensors under the shoe insole, based on Force Sensing Resistors (FSR) which gather the normal force that the user is exerting against the ground.

2.2 Comparison between eWalk and HiBSO

Both eWalk and Hip Ball-Screw Orthosis (HiBSO) are hip orthoses designed to assist hip flexion-extension but the HiBSO orthosis, being the predecessor, prioritized the user’s mobility, while the eWalk prioritizes being light.

The eWalk orthosis uses a high power servo motor aligned with the user’s hip as an actuated joint, while the HiBSO orthosis uses a ball screw in each leg that transforms the torque from a DC motor to a linear force applied to the thigh[38].



Figure 2.2: Comparison between the actuation systems used by both orthoses

The eWalk has no passive joints, and therefore, it does not allow hip motions in the sagittal plane nor rotations parallel to the longitudinal axis, excepting any motion due to the robot elastic structure, while the HiBSO orthosis had two spherical joints at each hip, which permit rotations around all 3 axis, allowing the user to perform flexion/extension, abduction/adduction and internal and external rotation. On the other hand, the eWalk orthosis weighs no more than 10 kg. Since all the structure has been manufactured with plastic and carbon fiber, it is much lighter than its predecessor, which needed several metallic parts for its leg mechanisms.

CHAPTER 3

Methodology

From the eWalk orthosis, as explained in section [2.1 Robot Design](#), we can only take 2 measurements: ground normal reaction forces using the sensorized soles, and the joint angular position using its encoders (integrating we can compute the angular velocity and angular acceleration, both of which will be used in section [5 Experiments](#)).

In other words, the only feedback we can receive for any control strategy relies on these 3 values.

We started from the approach taken by [39], where it was stated that a person carrying a weight could feel a reduction in the metabolic cost of walking if they were assisted by an exoskeleton. Therefore, we decided to experiment with torque based control strategies.

When using this kind of control, we send a pre-computed value of torque to the robot motors.

In this chapter we will discuss the several methods used to compute this value of the torque and different ways to mathematically model them in order to be able to be used by the optimizer.

3.1 Applying the biological torques of a healthy gait

Our first approach was to find the torque that the leg muscles apply to the hip joint along the lateral axis and try to directly apply it in the orthosis motors.

3.1.1 Healthy gait simulation

To obtain these values of the torque, the program used was called SCONE Software[40]. This particular application starts from the model of any moving creature (in our case, an anthropomorphic human model) and proceeds by setting some goals and a weight for each goal with weight being a constant value used to implement a kind of hierarchy among the goals) and choosing some variables as optimization parameters. The software then iterates these parameters and checks whether each of our particular goals returns us a better or a worse score. In the end, if the optimization variables and the goals have been set properly, a full simulation is obtained with a resulting gait and with the specific values of the chosen optimization variables. More information about this topic can be found in section [4.2 The SCONE optimizer](#) and in section [4.3 The SCONE cost functions](#)

For our particular case, the model used in SCONE was provided by the EPFL BioRob Laboratories. This model is based on [41], which states that human locomotion kinematics, kinetics and muscle activation of healthy human locomotion can be reproduced through a state-machine controller based on simple reflex rules. More details of the used model are available in section [4.1 The musculoskeletal model](#).

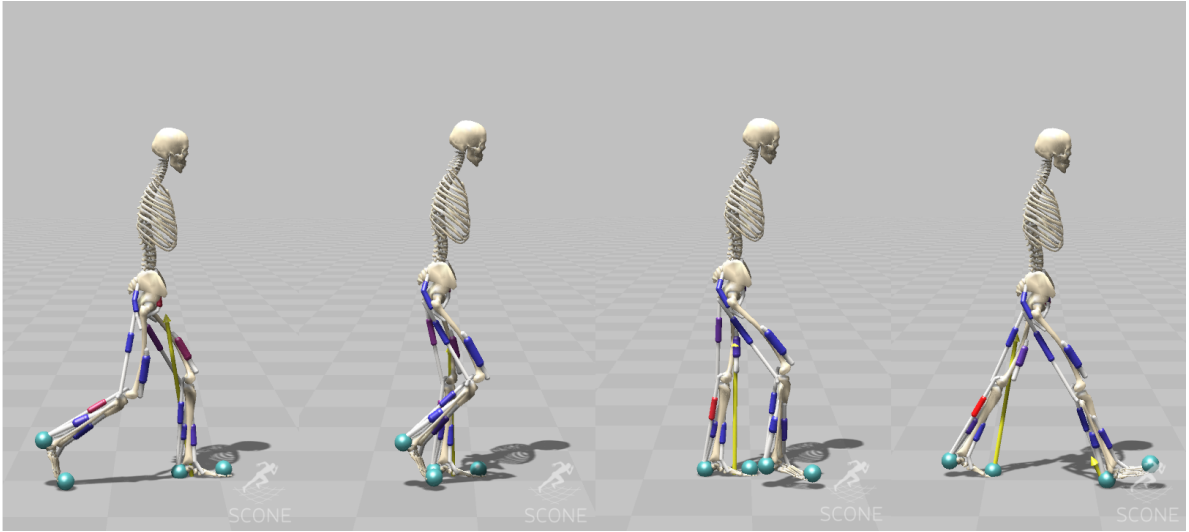


Figure 3.1: Depiction of the animation of our model in the SCONE Software[40] simulator, after running the healthy gait simulation.

At that point, we had a simulation of a healthy gait and we proceeded to analyse it, in order to find the torque that the leg muscles were exerting at the hip joint around the lateral axis. To do this, OpenSim Software[42] was used, and more specifically, the OpenSim Analyze Tool, which can easily measure the muscle forces and directions and return the desired torque in a simple and straightforward way.

Remember that we are constrained by the particular measurements we can gather from the real robot, meaning that we are not allowed to use values which would be known during simulations, if they can not be known on the real robot or the real subject. Therefore, we came up with two methods to detect the heel-strike: using the position and velocity measurements inside the motors or using the force ground sensors inside the shoes.

The first approach is based on experimentally finding the hip position and velocity during a heel-strike, using the motor encoders, and then looking for a moment when the hip position and velocity match the heel-strike ones. This particular approach was precarious since it presented a singular problem: each heel-strike is different from the previous one since the human walking is highly varied and inconstant.

In the Figure 3.2, we can see two curves showing the difference between the maximum and minimum values of the hip position and velocity obtained during the healthy simulation. In red, we can see the interval between the maximum and minimum values of the hip position and hip velocity during the heel-strokes.

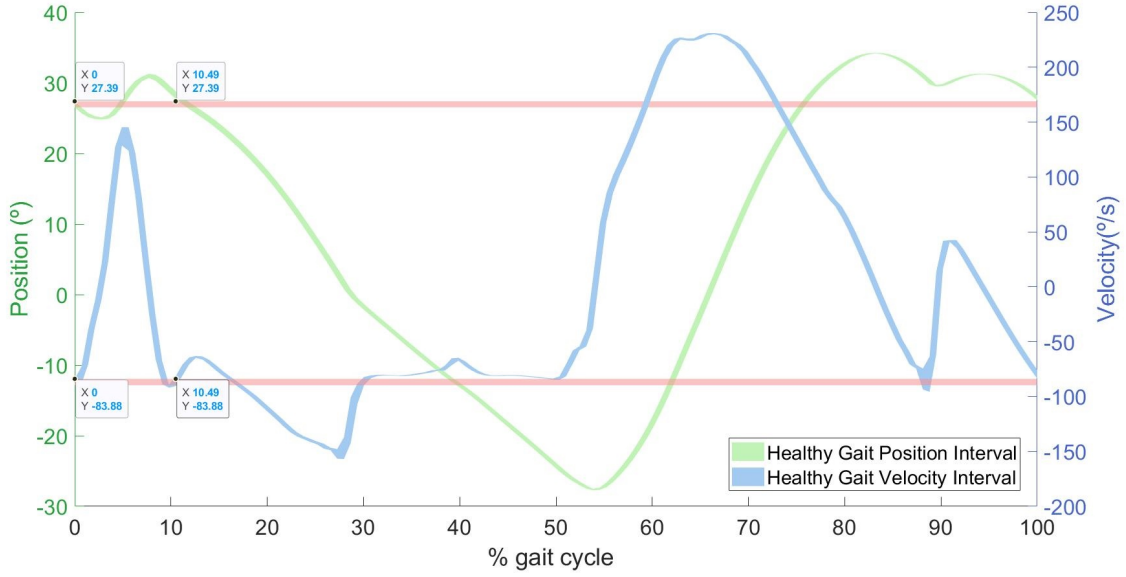


Figure 3.2: Graph with the values of the hip position and velocity during the whole simulation, where the red lines show the initial values of the position and the velocity, so we can easily see where the same value is repeated.

Looking at Figure 3.2, we can easily find a moment in time in which we would detect a false heel-strike, because the values of the hip position and velocity match, even though it is not a heel-strike. That being said, the method for detecting a heel-strike using the hip position and velocities is not simple to implement. It might require taking into consideration the position and velocity of the other leg, too.

No research work has been found regarding how to detect heel-strokes only using the hip kinematics. Other research works, such as [43], suggest that the knee joint kinematics are also needed, or [44], which proposes a method relying on computer vision, or [45], which uses an acceleration sensor and implanted EMG sensors on the sural nerve. The closest research work regarding how to detect heel-strokes using the hip angle is [46], which used hip angles and hip angular velocities, but also relied on using an accelerometer sensor.

In light of all of this, we considered detecting the heel-strike using the ground-force reaction sensors, which, in fact, is more robust and easy to implement.

At this point, using the heel-strokes, we could split our healthy gait simulation into steps and finally obtain a good biological torque profile, which we can see in Figure 3.3:

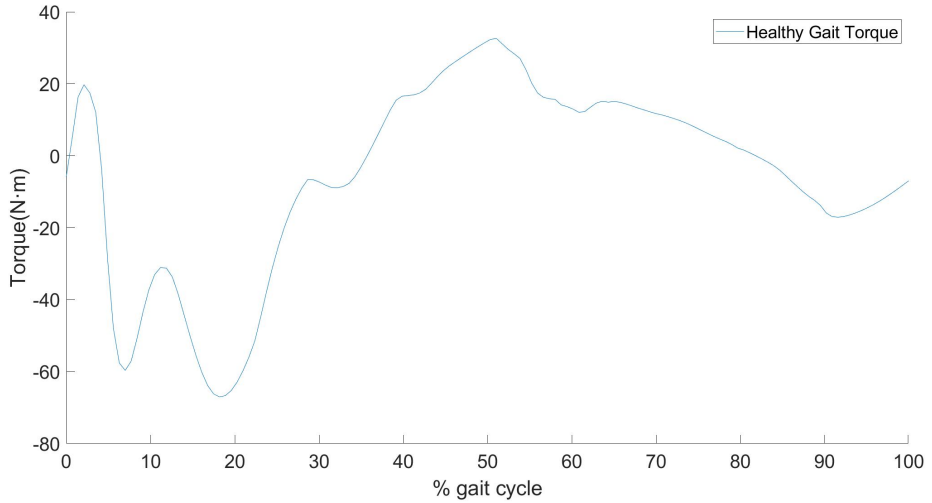


Figure 3.3: Biological torque profile that the muscles exert against the hip joint around the lateral axis.

Here we will also provide some plots, Figure 3.4, Figure 3.5 and Figure 3.6, depicting the activation of the main muscles involved in the hip flexion-extension motion when no assistance is provided. This data might be of use in the future to make comparisons with the cases presented in chapter 5 Experiments where the user does receive assistance. Remember that the activation is the measurement we use to have an idea of the energy consumption of the user in performing a motion as we explained in section 1.4 Simulation and neuro-mechanical models:

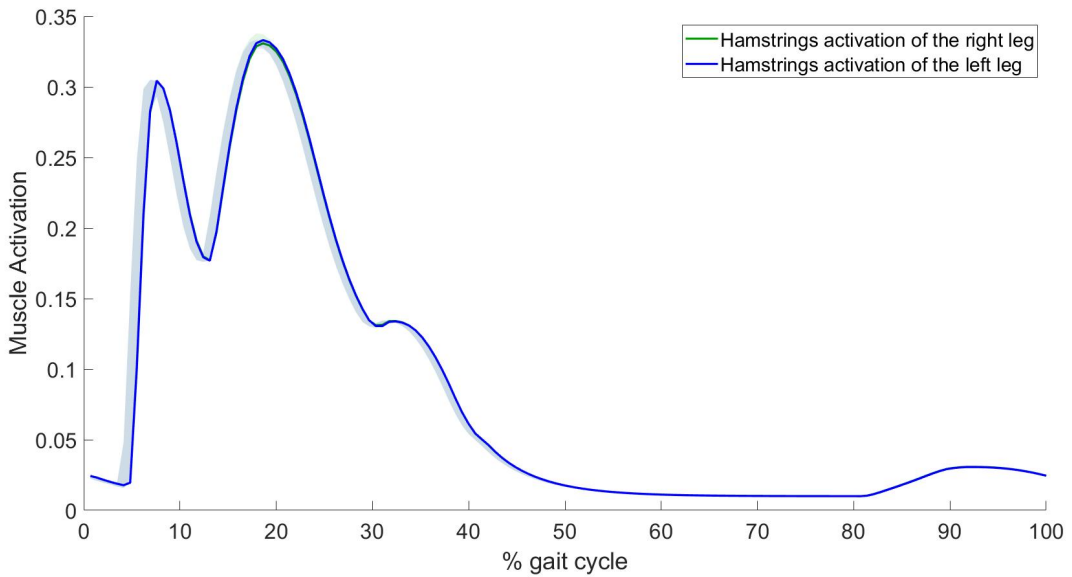


Figure 3.4: Representation of the activation signals of the hamstring muscles for the right and left legs, where the shaded area is all the range of obtained values, while the solid line is the obtained one once the walking had stabilized. Both legs have the same behaviour. Looking at the graphs it may seem that we only plotted one leg, but in fact, both legs have symmetrical behaviour therefore, the activation signals depict coincident profiles.

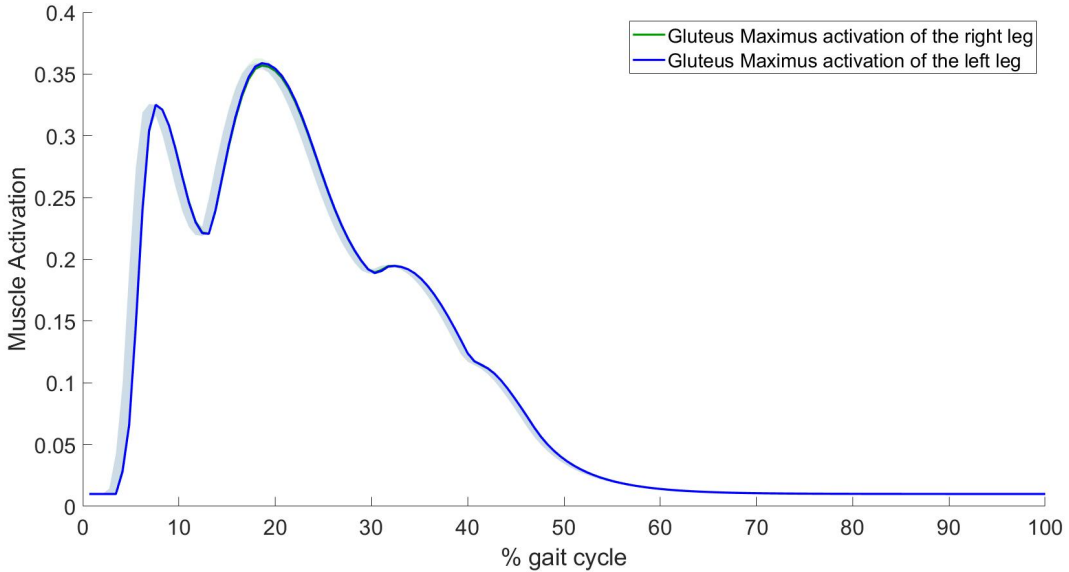


Figure 3.5: Representation of the activation signals of the gluteus maximus muscles for the right and left legs, where the shaded area is all the range of obtained values, while the solid line is the obtained one once the walking had stabilized.

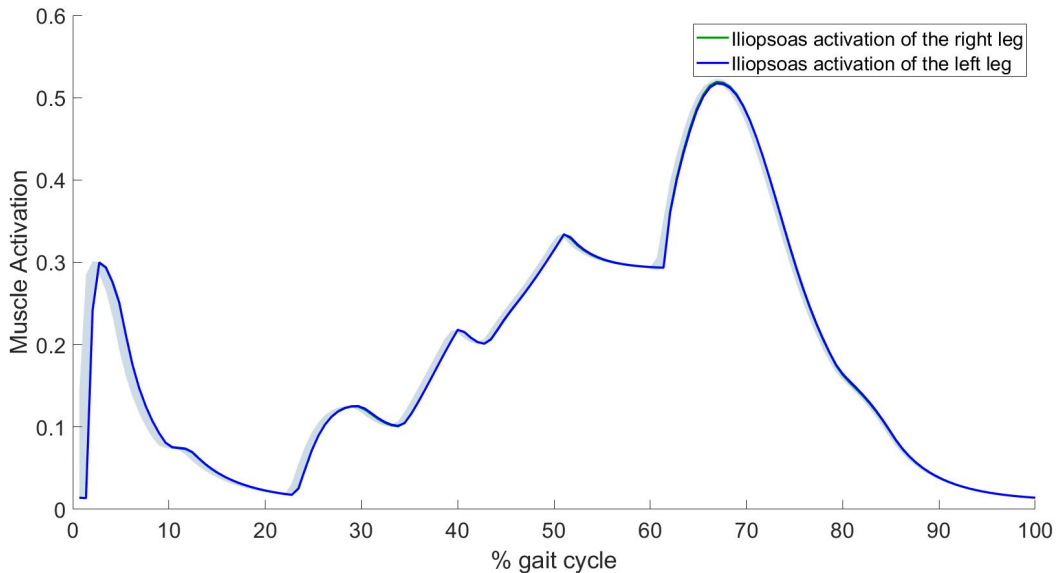


Figure 3.6: Comparison between the activation signals of the iliopsoas muscles between the motorized and non-motorized legs when using the Alpha torque profile, where the shaded area is all the range of obtained values, while the solid line is the obtained one once the walking had stabilized.

Remember that both legs have the same behaviour. As mentioned in the caption of Figure 3.4, looking at the graphs it may seem that we only plotted one leg, but in fact, both legs have symmetrical behaviour therefore, the activation signals depict coincident profiles.

As explained in section 1.4 [Simulation and neuro-mechanical models](#), the activation of a muscle is the measurement used to know the amount of energy consumed in performing a motion. Since we are working with a neuro-mechanical model based on reflex controllers, its virtual muscles are also activated using signals, which we can read and measure during simulations.

3.1.2 Mathematical model of the healthy gait

We wanted to feed the found torque profile into the SCONE Software[40] to see if our SCONE model had lower energy consumption with a torque aiding during the gait cycle.

The way the simulations were carried out was controversial. As indicated in section 1.1 Motivation the lack of strength in the muscles is due to a considerable amount of different aspects. Because of this, we took into consideration the possibility of the human body being asymmetric, resulting in the worst case scenario, where one half of the body is fully healthy, and the other one is not, generating in very unnatural motions. This particular case might not seem terrible for a human since half of the body is healthy, and therefore, he/she could walk, maybe with certain difficulties, but achieve reasonable walking. However, when talking about a non-symmetrical model inside of a simulator, it is extremely hard to achieve symmetrical walking. Therefore, when we say that we apply a particular torque to our simulations, we are stating that we will only apply it to one leg.

Our goal, from here will be to see if applying torque to only one leg, we can achieve a mostly symmetrical walking having less energy consumption for the group muscles of the motorized leg than the non-motorized one. More details regarding the model and the simulations can be found in section 4 SCONE Software Simulations and Methodology.

So as we stated at the beginning of this section, we want to feed our found torque into the simulation. To do this, we could take two approaches: Provide the torque profile point by point to the simulation depending on the gait percentage or the time, or model the shape into a mathematical equation.

Using the first approach has the advantage that we can feed a high-precision wave into the simulation, at the cost of the SCONE software[40] not being able to optimize its shape, meaning if there's a potential better shape, we would not be able to find it. On the other hand, using a mathematical model of the torque profile relied on having to approximate, but then the SCONE Software[40] would be able to optimize the wave parameters.

In consideration of all of this, we chose the second approach, allowing SCONE to optimize the shape of the torque profile. To do this, we used MATLAB Software[47], and more specifically the MATLAB Curve Fitting Tool, which allowed us to approximate a set of points into a curve.

Polynomial fit

Here, we chose the polynomial approach, because we could model a satisfying shape with just 5 variables using the polynomial equation of 4th degree.

$$T(t) = p_4 \cdot t^4 + p_3 \cdot t^3 + p_2 \cdot t^2 + p_1 \cdot t + p_0 \quad (3.1)$$

Where:

- $T(x)$ is the torque at the hip around the lateral axis.
- t is the time since the initial instant.
- p_4, p_3, p_2, p_1, p_0 are the polynomial coefficients.

As stated in section 4.1 The musculoskeletal model, our model has 64 inner optimization variables, and therefore has a low number of external variables to optimize which was adequate because the more variables the Optimizer has to manage, the more time it will need to run an Optimization. In Figure 3.7, the polynomial approximation can be seen:

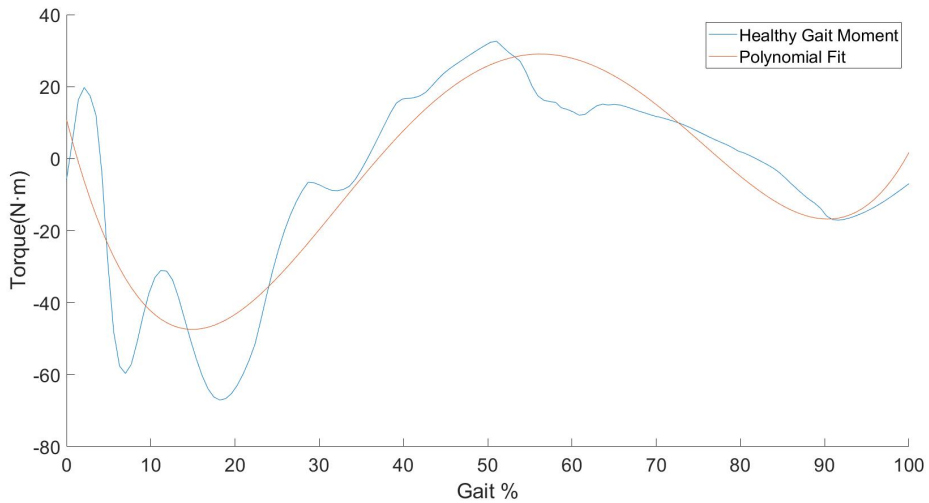


Figure 3.7: Biological torque profile that the muscles exert against the hip joint around the lateral axis along with its polynomial approximation.

At this point, the previous shape was used as an input for our SCONE model, with the polynomial function repeating every time the simulation detects a heel-strike. Here, in Figure 3.8 the signal received by the leg actuator for a particular simulation can be seen:

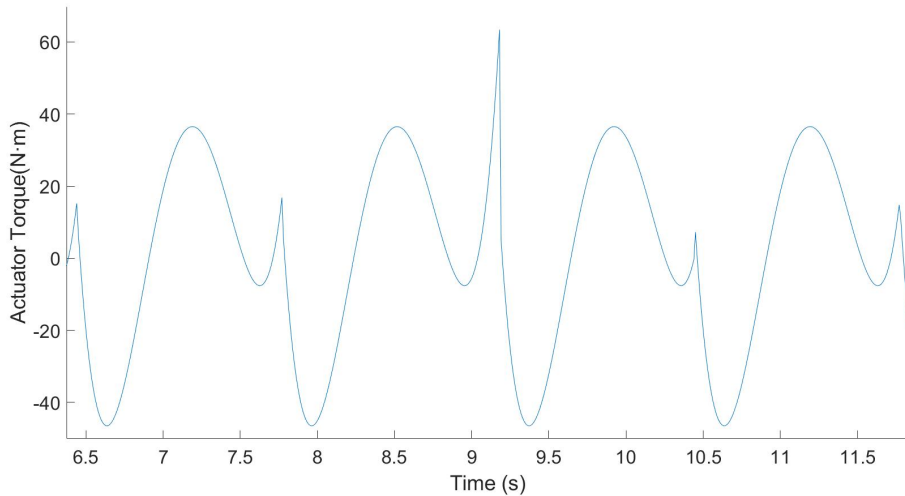


Figure 3.8: Signal received by the actuators using the polynomial function.

It is easy to see that the shape is not exactly as our function depicted, as some undesired overshoots appear. This happens because the duration of the step does not have the exact duration as the one we isolated using MATLAB, and because of that, its shape keeps growing if the duration of the step is longer than our original function or it gets truncated prematurely if the duration of the step is shorter.

One approach to solve this issue was to cut the wave when its end was reached as we can see in Figure 3.9:

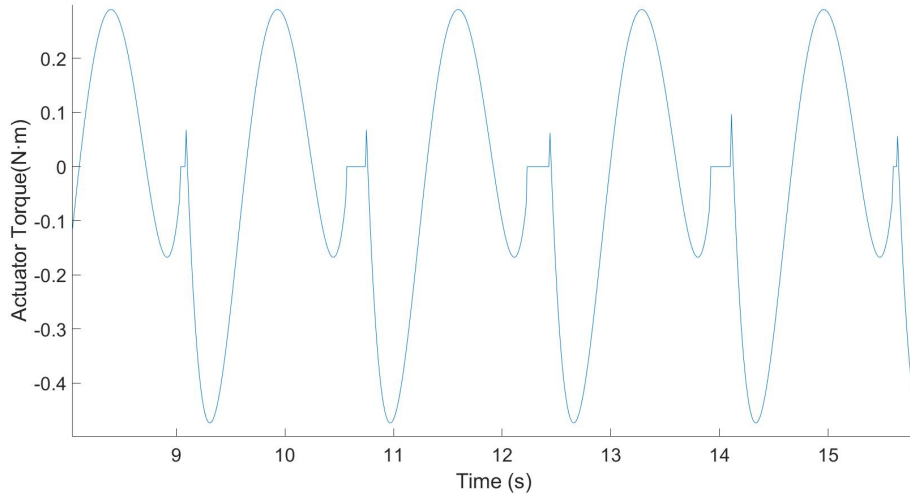


Figure 3.9: Signal received by the actuators using the polynomial function avoiding the function overshoots.

This solved the problem of having undesired overshoots, but according to [48][49], torque discontinuities may lead to sudden motions in the actuators and, therefore, problems in control, and because of this, many research works focus on getting rid of such discontinuities. In other words, a discontinuity in the torque drives a feeling of uncomfortable motion for the user and therefore should be avoided.

At this point, we saw that polynomial functions were problematic when trying to recreate a torque profile, because, in an ideal case, we needed to find a function that started and ended at the same point, a way to deal with a non-constant time between heel-strokes, and also take into account that SCONE Software[40] would not be allowed to optimize the polynomial coefficients in order to optimize the shape of the function (since a small variation in any of the coefficients of the polynomial might have canceled the condition of starting and ending at the same point).

Fourier series Fit

Since the polynomial approach did not fulfill our requirements, using Fourier series was taken into consideration. The main advantage of Fourier series (i.e. the sum of sine waves) compared to the polynomial approach, is that, by definition, Fourier series will always start and finish with the same value and also keep the properties of a periodic wave. That said, even if SCONE Software[40] changes any of its components during optimization, it will keep being appropriate for our purposes.

$$T(t) = a_1 \cdot \sin(b_1 \cdot t + c_1) + a_2 \cdot \sin(b_2 \cdot t + c_2) + \dots + a_n \cdot \sin(b_n \cdot t + c_n) \quad (3.2)$$

Where:

- $T(t)$ is the torque at the hip around the lateral axis.
- t is the time since the initial instant
- a_1, a_2, \dots, a_n are the amplitude of the different harmonics.
- b_1, b_2, \dots, b_n are the frequencies of the different harmonics.

- c_1, c_2, \dots, c_n are the angle offset of the different harmonics.

The period of the first harmonic, T_1 , is 1.4408s, i.e., the period of the steps when the model reached a stable gait.

Here, in the Figure 3.10, the Fourier series approximation obtained using MATLAB can be seen:

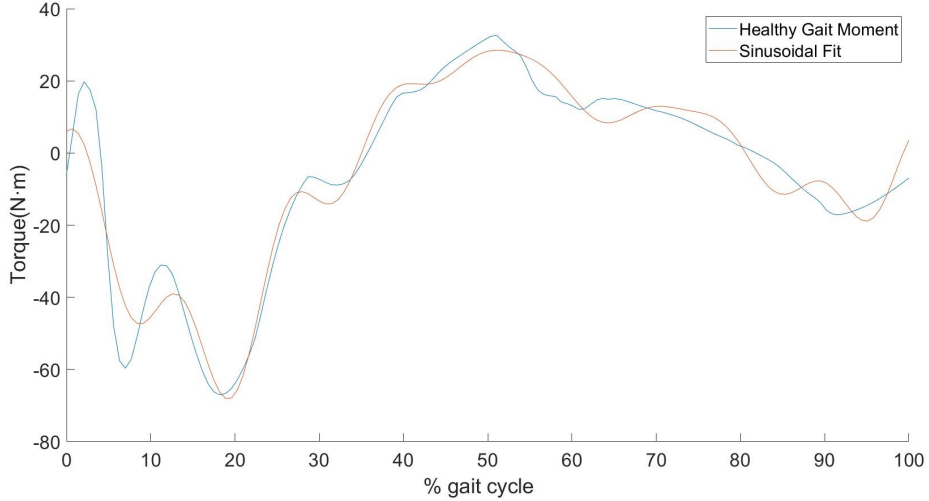


Figure 3.10: Signal fitting of the biological torque using Fourier series fitting.

Although, using this technique had two problems: Fourier series waves require more parameters than a polynomial wave, and therefore, the optimization will require more time. In fact, this particular wave has 8 harmonics, so we need up to 24 variables to parameterize it. Second, and more importantly, the Fourier series function is not robust against a change of frequency, meaning that if the user's walking is not constant, the frequency of the wave will have to change in order to match the frequency of the steps, otherwise there will appear discontinuities in the provided torque between steps.

In view of all of this, we had to come up with a method to chain sine functions with a varying frequency, and we found an algorithm that could compute the lacking or exceeding percentage of wave of our current hip torque profile:

$$\%P_n = \%P_{n-1} + \frac{t_n}{T_n} \quad (3.3)$$

Where:

- $\%P_n$ is the lacking or exceeding percentage of wave of the current step.
- $\%P_{n-1}$ is the lacking or exceeding percentage of wave of the previous step.
- t_n is the time elapsed between the initial and final heel-strokes for the current step.
- T_n is the period of the current hip torque profile wave.

With this equation we can compute the period of the upcoming hip torque profile:

$$T_{n+1} = \frac{t_n}{2 - \%P_n} \quad (3.4)$$

Where:

- T_n is the period of the upcoming hip torque profile wave.
- t_n is the time elapsed between the initial and final heel-strokes for the current step.
- $\%P_n$ is the lacking or exceeding percentage of wave of the current step.

This graphical representation in Figure 3.11 can be of use for better understanding:

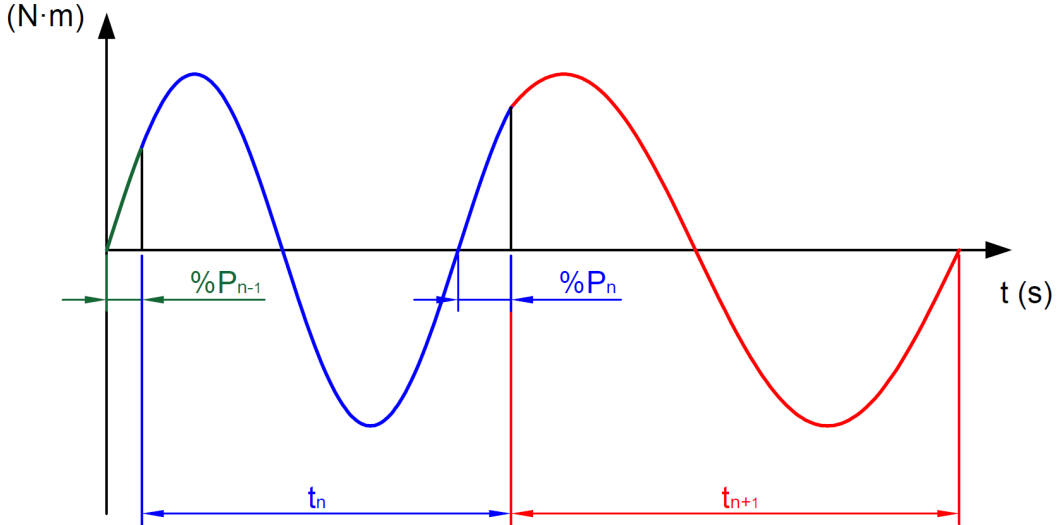


Figure 3.11: Graphical representation of the fusion between waves of different periods, where the green wave, represents a past wave, the blue wave, represent the current wave, and the red one represent the upcoming one. All of them with possibly different periods.

Using this algorithm, we can predict the period of an upcoming torque profile relying on the known data of the current and previous steps. This algorithm tries to match the end of a wave with the upcoming heel-strike.

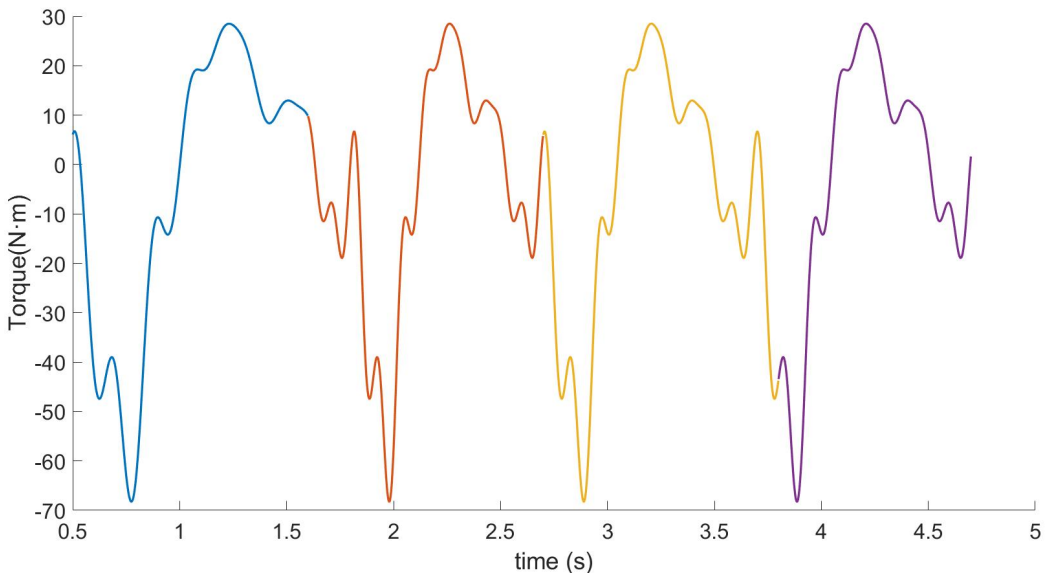


Figure 3.12: Example of four waves of different periods being perfectly chained using the mentioned algorithm. Each wave is depicted with a different color. We have no guarantee that the wave will start or end when it should, that is why the four waves seem to start or end at apparently random points. We can also see with a bare eye that some waves are wider, meaning they have a longer period, and on the other hand, if the wave is narrower, its period is shorter.

In Figure 3.12, we can see four waves of different periods which start and end at random points. Every time there's a change of wave (differentiated by different colors) simulated by a virtual heel-strike, the following wave, finishes the remaining previous wave (if any) and tries to match the predicted upcoming heel-strike.

Following from here, now that we were able to chain up waves of different periods, we tried optimizing the model in SCONE Software[40] using as an input for our actuator the previously found Fourier series function, working in harmony with the previously discussed algorithm.

The results were not satisfying. We achieved a very good and stable gait, but the motorized leg spent more energy than the non-motorized one. This is due to the fact that the model is very robust, and therefore, in order to obtain a good quality gait, in several cases, the hip motions opposed those of the motor.

Another aspect that has to be taken into consideration is that, as mentioned previously, the biological torque profile has 8 harmonics, and therefore, up to 24 variables.

If we take into account the Fourier series equations, we might know that the b parameter is related to the frequency of the particular harmonic, therefore, all the harmonic frequencies are multiple of the first harmonic one. Because of this, the b parameters do not need to be optimized, dropping the amount of optimization variables for this specific torque profile from 24 to 16, resulting in 8 amplitude a parameters, and 8 angle offset b parameters.

Even with the previous consideration, 16 variables are still too many, and sometimes the final obtained torque profile is completely wrong (remember that the model is robust enough to achieve a good walking with a horrible torque profile).

A great amount of the performed simulations resulted in cases where the motorized leg had a higher consumption than the non-motorized one, which, according to the purpose of our research work, should be considered as non-satisfying results. This happened due to the fact that the goals and measurements used by the simulator were not appropriate. The process of choosing, discarding and upgrading measurements and goal functions / target functions was one of the most time consuming tasks performed during this project.

In the Figure 3.13, the results of the last simulation using the biological torque profile can be seen:

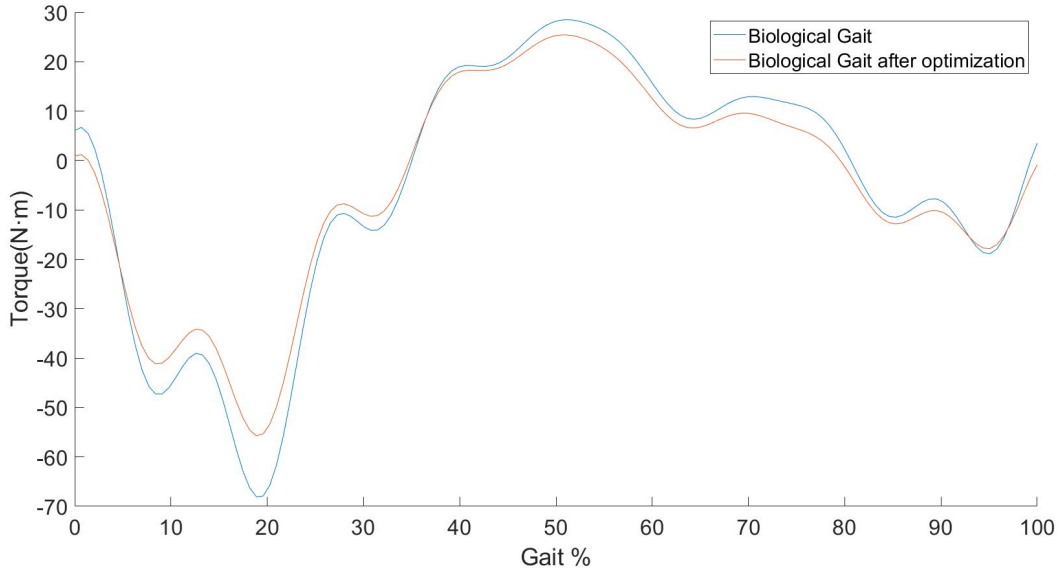


Figure 3.13: Comparison between the shapes of the original torque profile and the resulting torque after the optimization process.

As we can see, the shape of the torque profile is mostly unchanged (the biggest change is its amplitude), which means not a better shape was found using the previously defined goals. For this particular case we could see that the scores for the symmetric goal were close to 0, meaning that, indeed, we had a very symmetrical walking. Deeper definitions of the goals can be found in section [4.3 The SCONE cost functions](#).

On the other hand, the energy consumption scores, as previously mentioned, were not so good. Here we can see the comparison between the muscle activation of left and right legs:

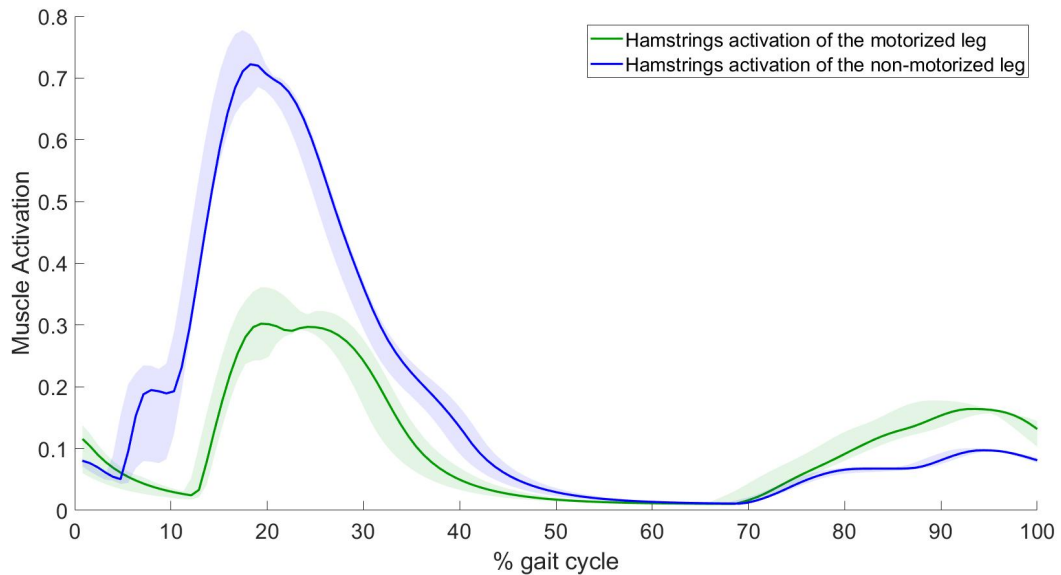


Figure 3.14: Comparison between the activation signals of the hamstring muscles of the motorized and non-motorized legs when using the optimized biological torque profile, where the shaded area is all the range of obtained values, while the solid line is the obtained one once the walking had stabilized.

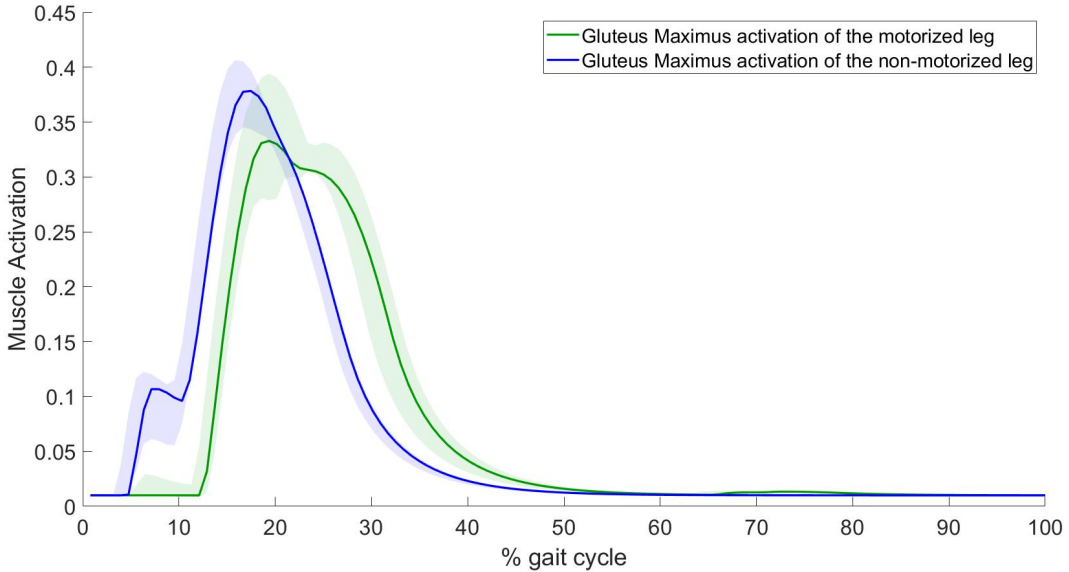


Figure 3.15: Comparison between the activation signals of the gluteus maximus muscles of the motorized and non-motorized legs when using the optimized biological torque profile, where the shaded area is all the range of obtained values, while the solid line is the obtained one once the walking had stabilized.

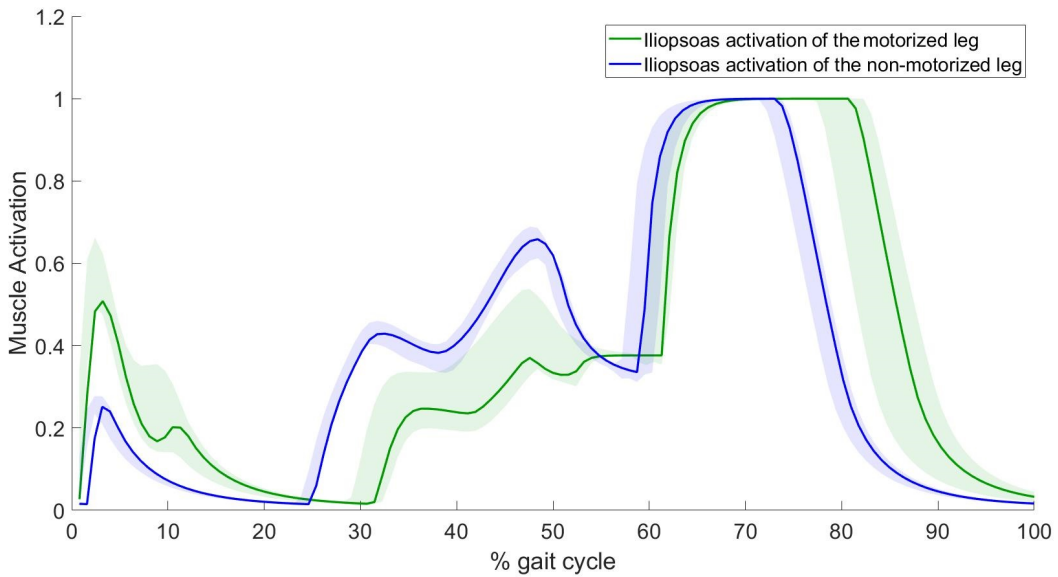


Figure 3.16: Comparison between the activation signals of the iliopsoas muscles of the motorized and non-motorized legs when using the optimized biological torque profile, where the shaded area is all the range of obtained values, while the solid line is the obtained one once the walking had stabilized.

As we can see in Figure 3.14, we indeed have a notable difference between the hamstring muscles, with only one muscle receiving assistance. We can observe in Figure 3.15 that the gluteus maximus muscle has a reduction of its peak value for the motorized leg with respect to the non-motorized one, but not a notable difference difference in matter of activation. And finally, and most importantly, for the iliopsoas muscles we can see in Figure 3.16 that the biggest peak for both legs is saturated at one, meaning that both legs are trying to exert the maximum force they are allowed.

Assuming that the motorized leg will have some kind of weakness, this kind of behaviour would be unacceptable, since we are demanding to the leg muscles that they perform at maximum capacity and for more time than the healthy leg's muscles.

So, because of this problem of having more activation for the motorized leg than for the non-motorized one, and due to the fact that the torque profile had 16 optimization parameters, meaning that trying to find a better shape for our torque profile would require much more computational time, our quest to find a proper torque profile using the biological one as a starting point was discontinued as a research approach.

3.2 Applying reference torques of a healthy gait

Since using the torques we computed did not work, we instead tried approaching the ones provided in the Workbook, which contains supplementary material for the article [20]. In this article, the author gathers data from a set of users during the walking cycle for a diverse set of speeds. To continue with the experiments, we used the hip torque profiles described in the mentioned paper, which rely on the weight and speed of the user.

Here, in Figure 3.17, we provide the shape of our fit torque profile:

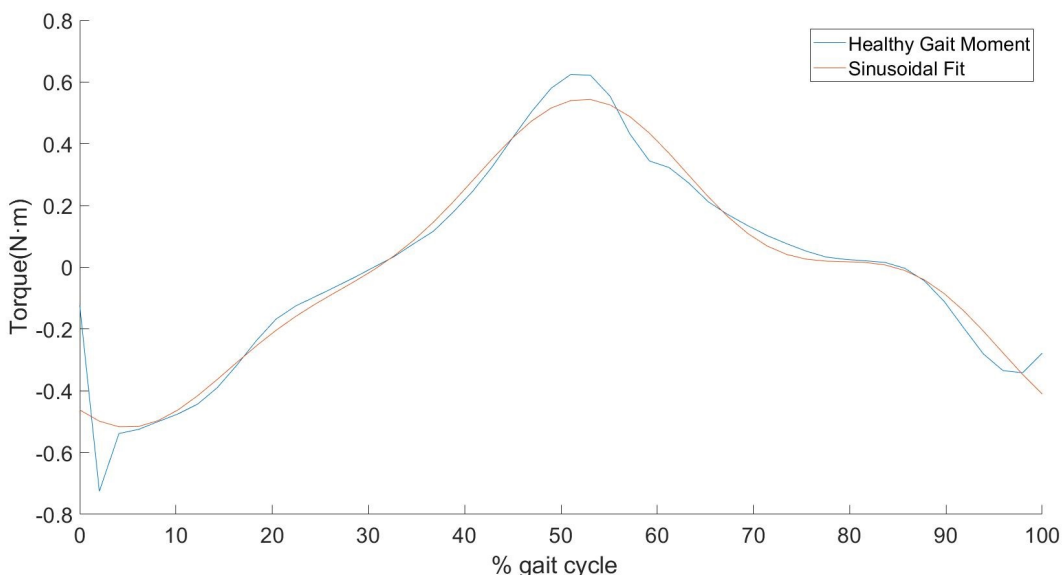


Figure 3.17: Torque profile obtained from [20], and its sinusoidal approximation.

As you can see with bare eye, the Fourier series approximation for this profile is simpler than the approximation we found for the biological Torques. In fact, this one only has 3 harmonics, which means that we need 9 variables to parameterize it, of which only 6 will be optimized.

When feeding this function as an input for the hip actuator in the SCONE simulator, the achieved results were more interesting. The quality of the gait was not so good, with evident anti-symmetric gaits, but clearly with a reduction in the metabolic cost for the motorized leg. More details and more information regarding torque profiles due to optimization and their implementation and results can be obtained in chapter [5 Experiments](#)

SCONE Software Simulations and Methodology

This chapter will provide a description of the model used to run the simulations and optimization, as well as a brief explanation regarding the SCONE Software[40] and the way it works. Also, the methods used to obtain a good performance from the mentioned program will be shown, including the definition and evolution of the used cost functions.

4.1 The musculoskeletal model

In this section we will describe the musculoskeletal model used for simulations:

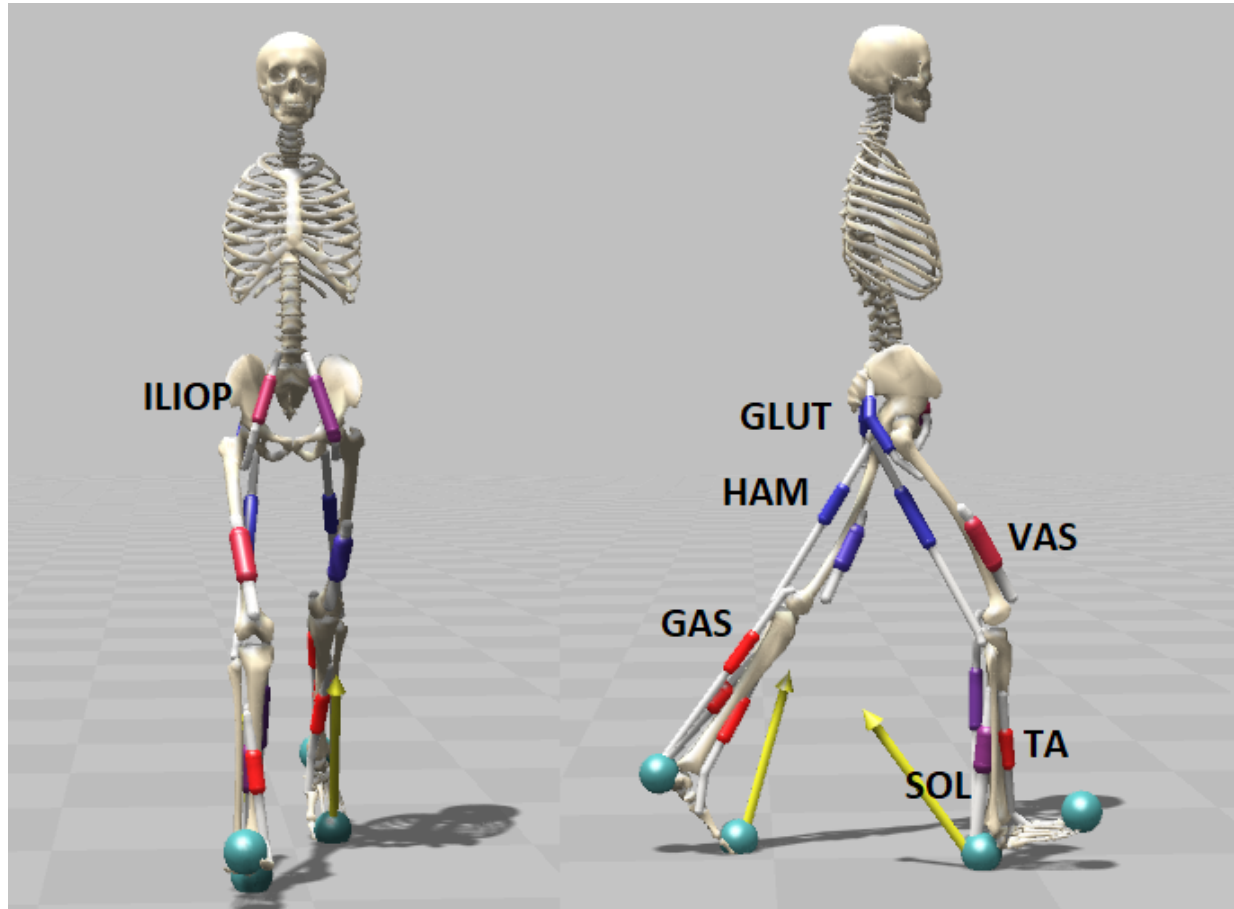


Figure 4.1: Musculoskeletal model used to simulate in SCONE Software[40], with the names of its muscles.

The model that was employed was adapted from [41]. It is composed of a skeleton of height = 1.8 m and weight = 75.16 kg. It has 9 DoFs in total. Three DoFs are needed to determine the position and the orientation of the pelvis, since the model movement is constrained in the sagittal plane, and other 3 DoFs for each leg, one for the hip, one for the knee, and one for the ankle.

Two spheres are attached to the feet to estimate the ground reaction forces using the contact model from [50] which states that we can compute the force between two bodies (in this case the ground and the feet) by measuring the deformation of a particular body (in this case the sphere) if we mesh its surface and we give elastic properties to that mesh. This being said, in Figure 4.1 we have two spheres per feet, one at the toes and one at the heel.

The model is also composed of 7 muscle-tendon units per leg: gluteus maximus (GLUT), hamstrings (HAM), iliopsoas (ILIPSO), vasti (VAS), gastrocnemius (GAS), soleus (SOL), and tibialis anterior (TA). The muscles are governed by a reflex controller trying to emulate the behaviour of the real human body, as we explained in section 1.4 [Simulation and neuro-mechanical models](#). As such, we have to take into consideration that the behaviour of each muscle varies, meaning each muscle will be stimulated differently, depending on if the particular leg where the muscle is located is in stance or in swing.

According to [51], the human locomotion bipedal model can be simplified into a point mass that travels on two massless springs. Despite its simplicity, this bipedal spring-mass model reproduces the dynamics of human walking.

In Figure 4.2, we can see different steps needed to obtain the current model according to the bipedal spring-mass model and what kind of reflex controller was intended for each muscle:

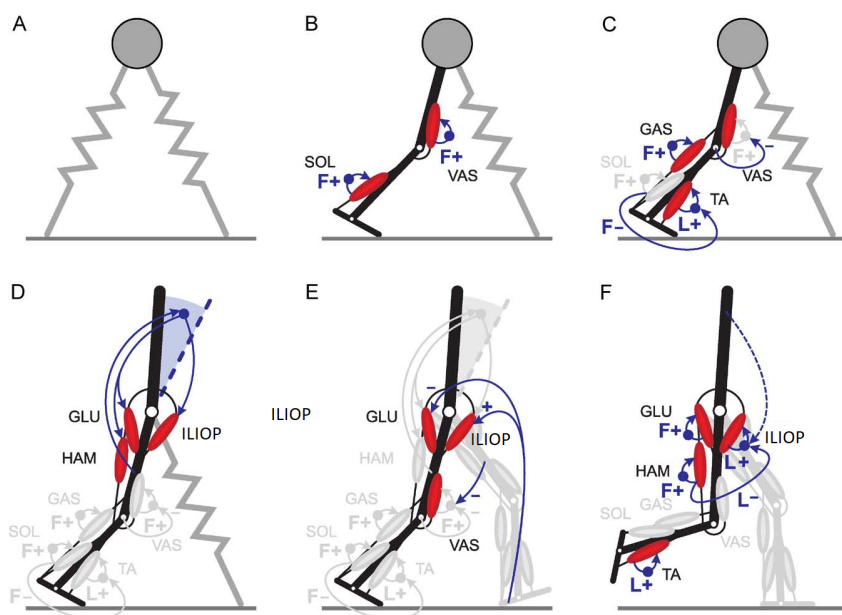


Figure 4.2: Evolution of the Geyer model, starting from the bipedal spring-mass model and developing by replacing the springs with muscles controlled by reflex stimulation, where A, B, C, D and E represent the muscles' behaviour during stance phase, while F represents the muscles' behaviour during swing.

Source: Adapted from Geyer, H., Herr, H. (2010). A Muscle-reflex model that encodes principles of legged mechanics produces human walking dynamics and muscle activities. *IEEE Transactions on Neural Systems and Rehabilitation*[41].

The controller governing each muscle is based on five different kinds of muscle stimulation based on reflexes, according to the implementation of [52]: positive and negative Force feedback (F), positive and negative Length feedback (L) and a Proportional Derivative feedback (PD) of the the trunk's forward lean angle.

The resulting model has up to 64 different optimization variables, and 3 different goals integrated within the model itself.

These 3 goals are:

- Gait quality.
- Gait effort.
- Limits of the human degrees of freedom.

The specific method in which this model has been parameterized and how these three goals return us a particular score can be found in [52]. As it is, the model is very robust and will always try to obtain good quality gaits; thus we will avoid making any changes.

As stated in section [3.1.2 Mathematical model of the healthy gait](#), we will use the model for two main purposes, to obtain a healthy simulation of human walking, from which we can extract a healthy torque profile for our legs around the hip, and for further optimizing the torque profiles we wanted to test with our model. Therefore, we have added two additional actuators to the original model.

This decision was taken for security reasons so in the future we do not have to change the model. But, in theory, the simulator will only use one of these two actuators, and consequently the other will never be actuated during simulations.

4.2 The SCONE optimizer

To run simulations and to optimize the previously presented model, we will use the SCONE Software [40].

Using this Software, a user can design control strategies, optimize a model along with a set of control parameters according to the user objectives, use an OpenSim model for predictive simulations and, finally, develop, optimize, and analyze predictive simulations.

The scone optimizer works using the Covariance Matrix Adaptation Evolutionary Strategy (CMA-ES) method. This method works by establishing some cost functions $f(x)$, and the objective is to find one or more candidate solutions making the value of $f(x)$ as small as possible[53]. This method is highly recommendable because it also implements a search costs function which will evaluate the efficiency of the optimizer method for exploring new solutions[54].

The quality of the optimization relies on the cost functions that the user defines. We will further discuss the different implemented cost functions.

4.3 The SCONE cost functions

The SCONE Software[40] cost functions, also called goals or measurements, are the utility that the simulator uses in order to know to what degree the simulation was good or bad.

Said this, we can define several types of goals or measurements and associate each one with a weight, where this weight is a constant parameter that will directly multiply the obtained score of a measurement. Therefore, they are used to give more or less importance to a particular cost function.

Secondly, we define a set of optimization variables. These optimization variables are variables that the optimizer will integrate in the Covariance matrix previously mentioned in section [4.2 The SCONE optimizer](#), and will keep iterating their values in order to obtain better scores. The chosen variables can be linked to anything that can be of use to us, for example the value of a variable from inside the model itself like the length coefficient of a muscle, or an auxiliary variable created by us like a gain that multiplies the torque exerted by an actuator.

When we create an optimization variable using SCONE Software[\[40\]](#), we have to determine an initial value for that particular variable and a range of values. Optionally, the software allows us to determine a standard deviation.

The optimizer will then try values inside the range and explore to a greater or lesser degree the borders of that range depending on how small or how large the value of the standard deviation is. Therefore, the optimization speed can be notably increased if those parameters are properly tuned.

When optimizing with SCONE it will always try to minimize the values of our desired goals (unless told otherwise), and more particularly, it will try to minimize the 3 goals integrated in the model, previously defined in section [4.1 The musculoskeletal model](#). These measurements have already been properly defined to obtain low values when the gait performance is good, and high values when the resulting gait is not satisfying.

4.3.1 Go as far as possible

Originally, with the first runs of our optimizing process , we only set one goal for the optimizer: We wanted the model to go as far as possible within our established simulation time.

Mathematically, we first defined it as follows:

$$P(x) = -x \quad (4.1)$$

Where:

- $P(x)$ is the obtained score for this particular goal.
- x is the position of the center of gravity of the user along the sagittal axis.

The problem with using this approach is that the optimizer obtained huge scores for this goal (in absolute value), ans therefore ignored the rest of the goals. So, we instead used the following one:

$$P(x) = 1/x \quad (4.2)$$

This meant that at the very beginning of the optimization we would have very large numbers, but the further we went, the smaller the score would become.

But this approach also offered us two problems: The optimizer could not deal with an infinite result in the case where the sagittal position of the body was 0, leading the simulation into an error. Secondly, if the model went back (but close to 0), the simulator returned a huge negative score, meaning that nothing motivated the model to go forward.

So finally, we used instead:

$$P(x) = \max \left(\min \left(5, \frac{1}{|x|} \right), \frac{1}{5} \right) - \frac{1}{5} \quad (4.3)$$

Where the “min” operator, avoids the infinite values when the sagittal position of the body is 0 while the “max” operator prevents the body from going backwards. When both conditions are met we can achieve good results, avoiding huge scores that would outrank the other goals.

We ran the simulation, setting the previous goal, and setting a duration for simulations of 1 minute. Therefore the SCONE Software[40] started the iterating process of optimizing until it stopped (the optimizer automatically stops when after some iterations, we are unable to achieve an improvement on the final score, or until the amount of iterations for a particular optimizing process reaches a specific value).

4.3.2 Torque minimization

Since we have an active hip actuator, we add a torque minimizing goal to try to make this torque as efficient as possible. In other words, we want this torque to be as small as possible just for energy efficiency reasons. We also give it the lowest possible weight, since if it goes higher than other more important goals, the optimizer will simply reduce this torque to 0 (which would make the optimization process itself redundant, since we are looking for good torque profiles).

4.3.3 Torso tilt

This goal was meant to make the model remain straight. In multiple simulations, the model performed strange motions and used the torso to keep its balance, resulting in completely unnatural motions, with unsuccessful gaits.

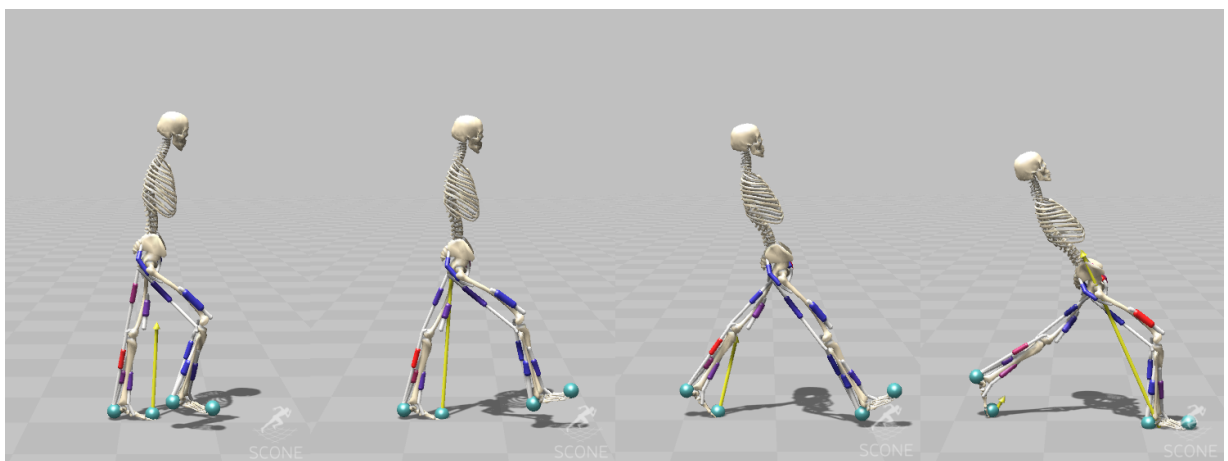


Figure 4.3: Depiction of the SCONE model falling back before implementing the Torso tilt constraint.

This goal sets a range for the torso inclination with respect to the sagittal plane. Every time the torso gets out of that range, it receives an instant penalization, which normally, automatically

discards the simulation due to the bad score.

4.3.4 Toe-strike

At this stage, we realised that multiple simulations failed when, at a given point, the model landed with the Toe instead of landing with the heel. This happened several times at the end of the simulation, because the simulator was trying to make its last step less energy consuming. Consequently, we were not able to achieve stable walking, since the simulator's purpose was to make the model fall at the very end.

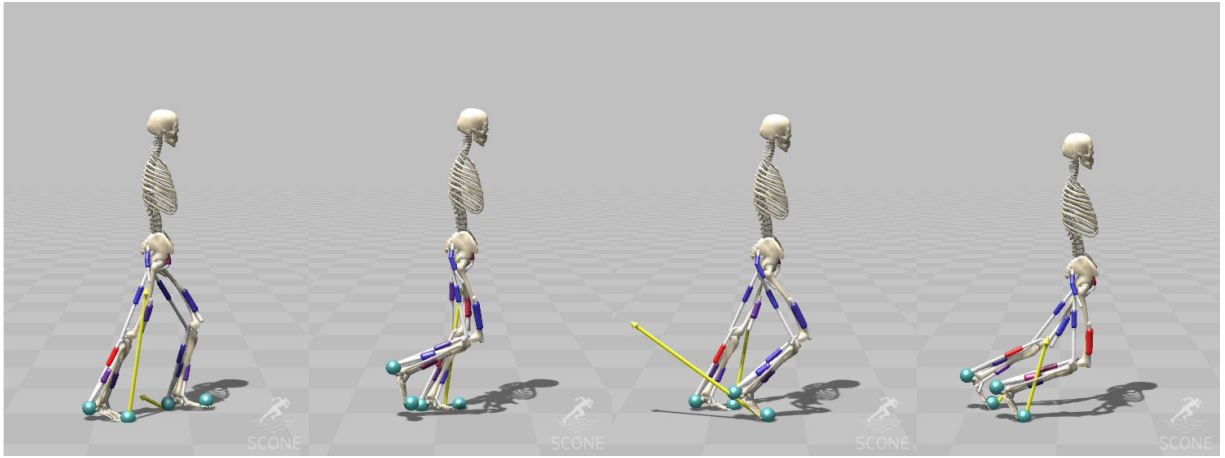


Figure 4.4: Depiction of the SCONE model landing with the toe before implementing the toe-strike constraint.

To avoid this, we added a simple goal: if at any moment of the simulation, we detect a toe-strike, add a huge handicap to the simulation. In our case, we added 10000 to the final score if that happened (remember that we want to minimise).

As we stated in section 4.1 The musculoskeletal model, the model can measure the force between the ground and the feet using four virtual spheres (two per feet), one located at the heel and one located at the toes. Therefore, to model this condition, we implemented a simple state machine: Supposing we observe one of the two legs, starting from stance, when we detected no force from the spheres of its foot, it means that that particular leg has switched to swing. If then we detected force in the heel sphere before detecting it in the toe one, it means we have landed properly. Therefore, the state machine switches to stance again; if, on the other hand, we detect a force at the sphere of the toe before detecting it at the heel, it means the leg has landed with a toe-strike.

4.3.5 Symmetric walking

We created 2 goals to make the simulator try to keep the symmetry between the steps of both legs:

The first one was to compare the hip angles of both legs for each step. To do so, we obtain a score by checking, every time we detect a heel-strike, the difference between the hip angles of the just-finished step and the previous step of the other leg (since we cannot use the current step because it is still ongoing) for every particular time iteration.

$$P = \sum_{n=0}^{R_s} \left(\sum_i (\theta_{R_n i} - \theta_{L_{n-1} i})^2 \right) + \sum_{n=0}^{L_s} \left(\sum_i (\theta_{L_n i} - \theta_{R_{n-1} i})^2 \right) \quad (4.4)$$

Where:

- P is the obtained score for this particular goal.
- θ_R and θ_L are the hip angular position of the right and left leg respectively.
- R_s and L_s are the amount of steps of the right and left leg respectively.
- n is the current step being evaluated.
- i is the set of all time iterations for each step.

The second one was to compare the lengths of the right and left steps to assess whether or not they were equal. The score is simply calculated by computing the difference between the current finished step and the last step of the other leg every time we detect a heel-strike.

$$P = \sum_{n=0}^{R_s} (l_{R_n} - l_{L_{n-1}})^2 + \sum_{n=0}^{L_s} (l_{L_n} - l_{R_{n-1}})^2 \quad (4.5)$$

Where:

- P is the obtained score for this particular goal.
- l_R and l_L are the length of the steps of the right and left leg respectively.
- R_s and L_s are the amount of steps of the right and left leg respectively.
- n is the current step being evaluated.

This second goal or measure might seem redundant because if the angles of the hip are symmetric, the length of the step will also be, but in reality this was an easier condition to accomplish and therefore the simulator first tried to accomplish equal step lengths and then equal leg angles.

In both equations we use the difference of the squares to avoid having different scores due to positive or negative values.

4.3.6 Less consumption for the motorized leg

When we arrived at this point, we realised that the simulator took a great deal of time to reach a point where the torque was synchronous with the gait cycle. The model is very robust, and given enough time, it will always return a stable gait if no goal or measure has a higher priority than the three goals inside the model itself, which allow the simulation to obtain a good quality gait. Therefore, in multiple simulations, we obtained a torque profile that might oppose the user at given moments. This resulted in having greater consumption for the motorized leg than for the non-motorized one, which is the exact opposite of our final objective. In consequence we created this function to force the simulation to have less consumption for the motorized leg than for the non-motorized one.

To measure the energy consumption of a particular muscle group, we measured the amount of

activation signal as explained in section [1.4 Simulation and neuro-mechanical models](#). Therefore, to know if one leg is consuming more energy than the other, we simply compare the activation signal of each muscle group of one leg with those of the other leg.

$$P = \sum_i ((a_{G_m_i} - a_{G_n_i}) \cdot K_G + (a_{H_m_i} - a_{H_n_i}) \cdot K_H + (a_{I_m_i} - a_{I_n_i}) \cdot K_I) \quad (4.6)$$

Where:

- P is the obtained score for this particular goal.
- a is the activation signal of a particular muscle group (G , H or I) of the motorized or non-motorized leg (m or n) for a particular time iteration (i).
- G , H and I represent each of the muscle groups involved in the hip flexion extension, namely the gluteus maximus, the hamstrings and the iliopsoas.
- m and n represent the motorized and non-motorized leg respectively.
- K_G , K_H and K_I are the particular gain that we apply to each muscle group.
- i is the set of all time iterations during all the simulation.

As we can see in the equation, each muscle group is controlled by its particular constant gain (K_G , K_H and K_I). This is because some muscle groups have larger activation than others. Because of that, the simulator only focused on the group with the largest activation, sometimes resulting in an increase on the groups with an apparently less significant activation. Therefore, we added this gain to try to compensate the difference between all three muscle groups. The final gains have been found experimentally because the criteria used by the program to give more priority to a given muscle group than to another was unpredictable. The final gain values are presented here:

- $K_G = 0.75$
- $K_H = 1$
- $K_I = 1.5$

We have to point out that it is the only equation that can achieve a negative result. This will happen when the activation of the non-motorized leg is higher than the activation of the motorized one, so, in fact, we want it to be negative. But because of this we have given it a very small weight compared to any other measurement, to actively try to avoid it rapidly outscoring any other goals.

We have to mention, however, that this particular equation really meant a difference in the simulations. It notably decreased the amount of time needed for the simulator to obtain a valid result, and also the final torque profile obtained was more satisfying than the ones obtained before.

4.4 Simulator approach

In this section we will discuss the behaviour of our model obtained through optimization, and the approach taken to implement the control strategy.

As discussed in section [3.1.1 Healthy gait simulation](#), our control strategy is based on detecting the heel-strokes of the user, or more accurately, measuring the time between the heel-strokes. Then we apply the particular torque profile we are testing to the simulator, and for each step we may compress or expand this torque profile. To this we chain the different torque profiles for each step with one another depending on the walking speed of the user.

The way the controller works is by starting to assist the user after two steps (one stride). The first non-assisted stride is used to compute the period of one of our steps and thereby compute the shape of the upcoming torque profile.

We have observed that the first steps are always anomalous, meaning that the first steps of all simulations are very different from the ones obtained after a few seconds, when the walking becomes more stable. Because of this, we have implemented a proportional control loop that makes the changes in the current period have less repercussion in the upcoming period in case they are too anomalous:

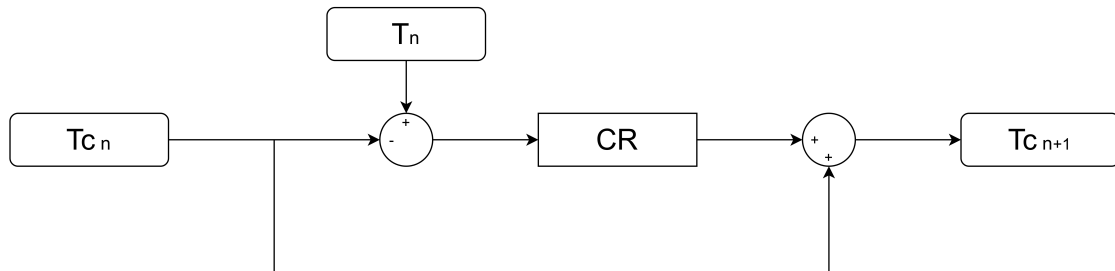


Figure 4.5: Block diagram of the proportional control loop used to make the model more robust against drastic changes in the torque

$$T_{c_{n+1}} = (T_n - T_{c_n}) \cdot CR + T_{c_n} \quad (4.7)$$

Where:

- $T_{c_{n+1}}$ is the desired period for the upcoming step.
- T_n is the real measured period of the current step.
- T_{c_n} was the desired period of the current step.
- CR is the proportional variable which we call “Control Ratio” which determines the influence of the error between the desired torque and the real measured one.

For the simulations we will use a $CR = 0.5$, since the walking always will start with this anomalous behaviour. During experiments, we will use a different value. Section [5.1.2 Experiment details](#) can be checked for further information.

Here, in [Figure 4.6](#) we can see an example of the behaviour of the walking period for a random simulation:

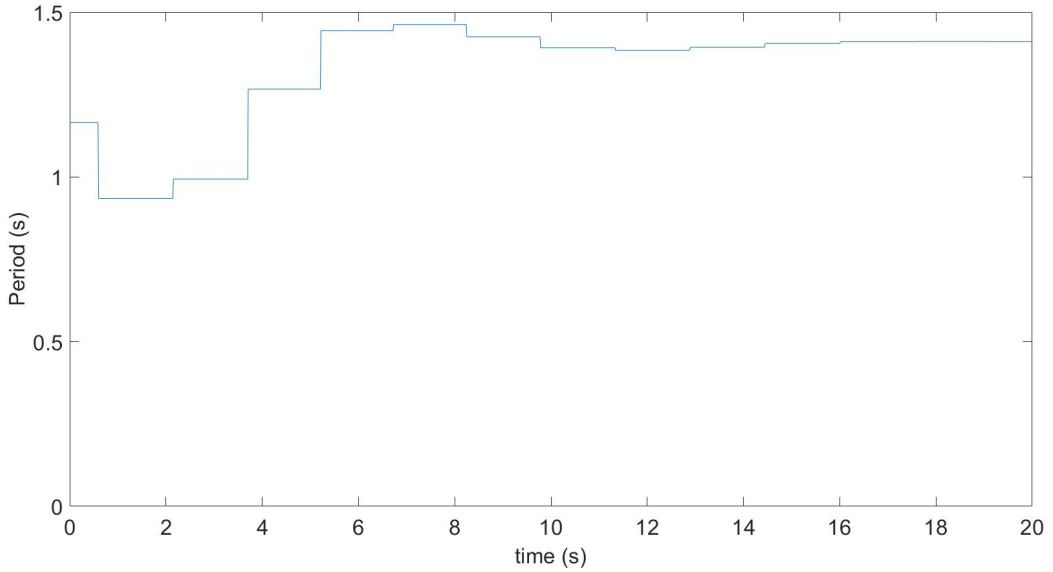


Figure 4.6: Graph depicting the behaviour of the period for a random case.

As we can see, the gait is not steady, and because of that, we have large variations within the period, but each step takes us closer to the convergence.

This period is not computed until we detect two heel-strikes with the motorized leg, therefore we require an initial guess of the period in order to start this iteration process. We have experimentally seen that a good guess for this first period is using the same period as first harmonic of the defined torque profile, which matches the period of the biological gait that we gathered at the beginning of our research project, or in mathematical notation:

$$T_0 = \frac{2\pi}{b_1} \quad (4.8)$$

- T_0 is the period of the first torque profile received by the motor.
- b_1 is the frequency component of the first harmonic of the provided torque profile.

CHAPTER 5

Experiments

In this chapter we will display the procedure and results of testing the obtained control strategies, with real subjects.

5.1 Experiment approach

In this section we will describe the experiments, and some technical details regarding how they were carried out.

5.1.1 Experiment description

The experiments were based on equipping a subject with the eWalk orthosis and having him/her walk on a treadmill at a constant speed.

An experiment had two parts: During the first part of the experiment we will had the user walk without providing any assisting torque. This first part was of use to us to have a reference pattern of the walking gait of the user. During the second part of the experiment, we applied the required assistance based on the particular strategy we found by running optimizations on the simulator. Finally, we analysed the obtained data and asked for the subjective opinion of the user regarding the assistance received.

Some useful data analysis was run according to the obtained results:

- Comparing the differences between the torque we obtained through optimization and the real torque applied by the actuators.
- Comparing the hip angles between the first part and the second part of an experiment, to check if there was any serious alteration in the user's gait when receiving assistance.
- Comparing if the torque profile was in sync with the hip acceleration, to know if it was assisting when it should.

Here in Figure 5.1 we can see a user walking over the treadmill during an experiment:

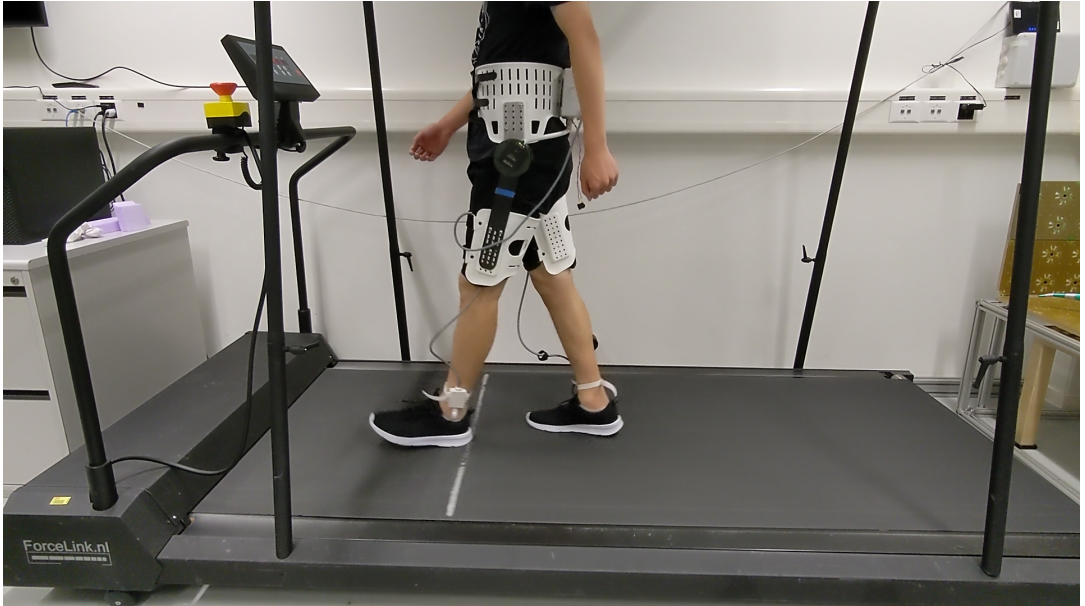


Figure 5.1: Picture of a subject walking on a treadmill while wearing the eWalk orthosis.

We have to mention, that since we couldn't find a user with one healthy leg and a unhealthy one. Because of this, the controller will be tested on healthy users, and we will apply the found torque profile at both legs using two independent loops, allowing asymmetrical walking.

The lab was only equipped with one device which could allow us to measure the energy consummation of the user. The mentioned device was a heart-rate sensor that the users were intended to wear during experiments but its readings showed that the heart-rate of a human is heavily influenced by multiple factors, such as stress, agitation, or even something as subjective as being nervous, rather than just the user's level of fatigue. Because of this, no real energy consumption measurements were taken, and the only feedback received, as mentioned before, came from the subjective opinion of the user regarding his/her own experience during the experiments.

5.1.2 Experiment details

The torques provided during the experiments were always tested first by increasing the percentage of assistance progressively. By doing this, we could make sure that the torque was in the correct direction and that the user was feeling comfortable before proceeding with the experiment. For safety reasons, the eWalk orthosis was equipped with an emergency button (as seen in section [2.1 Robot Design](#)) and also the controller could be quickly turned off remotely, if needed.

In chapter 4 it was mentioned that we apply a “Control Ratio” when we try to predict the period of the upcoming step. The problem is that in real life, humans do not tend to have a stable walking like we observed in our model during simulations, meaning that the simulator tended towards a periodic walking, while the walking of a real human can have slightly different periods. Because of this, it made no sense to implement a control strategy to avoid great variations in step frequency.

Because of this, during experiments, this “Control Ratio” was set to $CR = 1$, which in mathematical notation translates to:

$$T_{c_{n+1}} = T_n \quad (5.1)$$

- $T_{c_{n+1}}$ is the desired period for the upcoming step.
- T_n is the real measured period of the current step.

This value for the “Control Ratio” was found experimentally through trial and error, but it has to be mentioned that the controller was never in perfect synchronization with the user for any other value of CR showing some unexpected discontinuities in the provided torque profiles.

Another important difference between the implemented controller and the one used in simulation was the varying amplitude of the torque profile depending on the user’s speed. As mentioned in section [1.2.1 Gait kinematics and dynamics](#), the torque required for walking for each articulation depends on the user’s particular speed.

When we were working with the simulator, the optimizer could freely change the amplitude of each of the harmonics, resulting in drastically increased or reduced torque, if needed. Since the simulator always tended towards a constant speed, the optimizer tried to find a good torque profile to match that particular speed.

For humans subjects, on the other hand, this no longer applied. Each user had a different stature and physiognomy, and even though all the subjects were supposed to walk on the treadmill at the same speed, there was not a fast nor simple way to convert between frequency of the steps of the users to a real walking speed, therefore, there was not an objective method to determine if the user considered his/her walking speed to be slow or fast

Therefore, a simple method was applied to increase the assisting torque that the user would receive from the orthosis which depended on the relation between the frequency of his/her steps and the frequency of the steps used during simulations. The faster the controller detected a heel-strike, the higher the provided torque was.

$$K_T = \frac{f_n}{f_0} = \frac{T_0}{T_n} \quad (5.2)$$

Where:

- K_T is the proportional gain we apply directly into the provided torque.
- f_n is the frequency of the current step of the user.
- f_0 is the frequency of the period of the original torque profile used in simulations.
- T_n is the real measured period of the current step.
- T_0 is the period of the original torque profile used in simulations, as explained in section [4.4. Simulator approach](#).

Also we have to take into consideration that just applying this computed gain as soon as a heel-strike was detected, would have created a discontinuity, and according to section [3.1.2 Mathematical model of the healthy gait](#), discontinuities along the torque should be avoided. So we also applied a proportional control loop that would raise the value of K_T during a fraction of one step, in order to have the desired torque at the end of it.

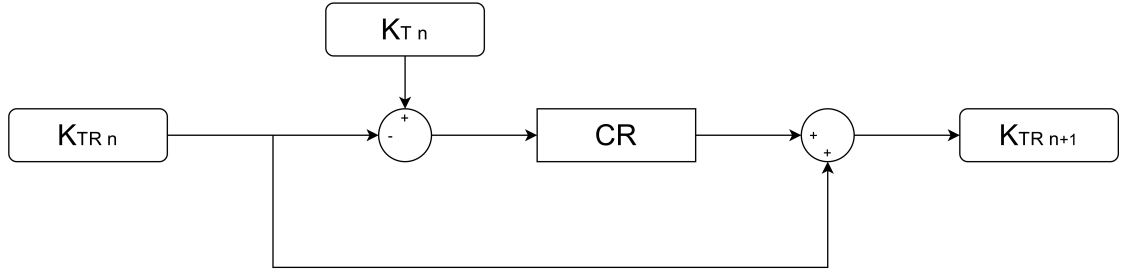


Figure 5.2: Block diagram of the proportional control loop used to make the current gain of the torque signal sent to the motors converge to the desired value.

$$K_{TR_{n+1}} = (K_{T_n} - K_{TR_n}) \cdot CR + K_{TR_n} \quad (5.3)$$

Where:

- $K_{TR_{n+1}}$ is the multiplier for the torque sent to the motors for the next time iteration.
- K_{TR_n} is the current multiplier for the torque sent to the motors.
- K_{T_n} is the desired torque multiplier.
- CR is the proportional variable which we call “Control Ratio” which determines the influence of the error between the desired gain and the current one.
- n is each one of the time iterations.

The Beagle-bone integrated inside the robot which ran the program that controlled the orthosis, executed all the loops at a frequency of 500 Hz, or in other words, every 2 ms. Taking into account how often the loop executes, and how fast the users walked on the treadmill, the value of CR was experimentally set to $CR = 0.0001$ which presented an adequate convergence time for such a fluctuating variable as the walking period.

5.2 Alpha experiment

The first experiment was using the first torque profile obtained through the simulator that presented less energy consumption for the motorized leg than for the non-motorized one.

5.2.1 Simulation evaluation

As a matter of practicality, to avoid confusion, we will refer to this experiment as the Alpha experiment. Also, we will refer to the provided torque profile as the Alpha torque profile.

Here, in the following Figure 5.3, we can see its shape obtained using the optimizer:

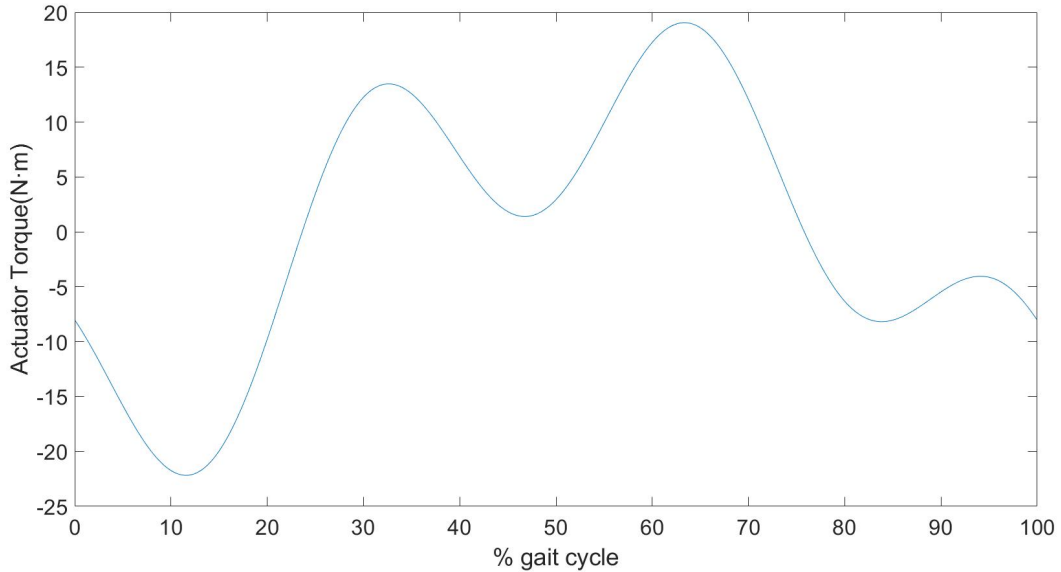


Figure 5.3: Shape of the Alpha torque profile, obtained using the simulator.

Below, we will provide the comparison graphs of the activation signals received by the muscle groups between the motorized and the non-motorized legs, obtained during simulations:

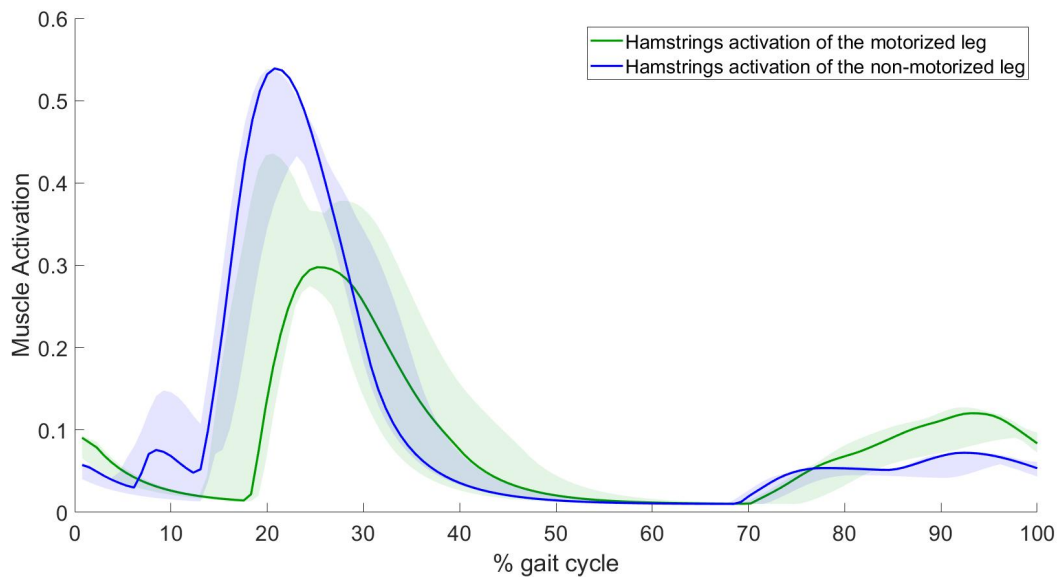


Figure 5.4: Comparison between the activation signals of the hamstring muscles between the motorized and non-motorized legs when using the Alpha torque profile, where the shaded area is all the range of obtained values, while the solid line is the obtained one once the walking had stabilized.

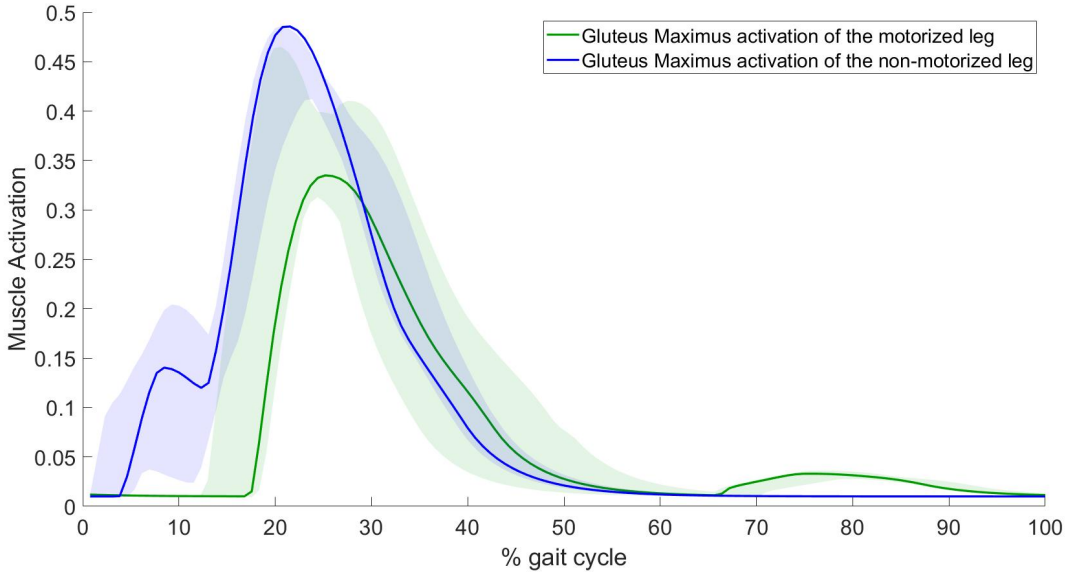


Figure 5.5: Comparison between the activation signals of the gluteus maximus muscles between the motorized and non-motorized legs when using the Alpha torque profile, where the shaded area is all the range of obtained values, while the solid line is the obtained one once the walking had stabilized.

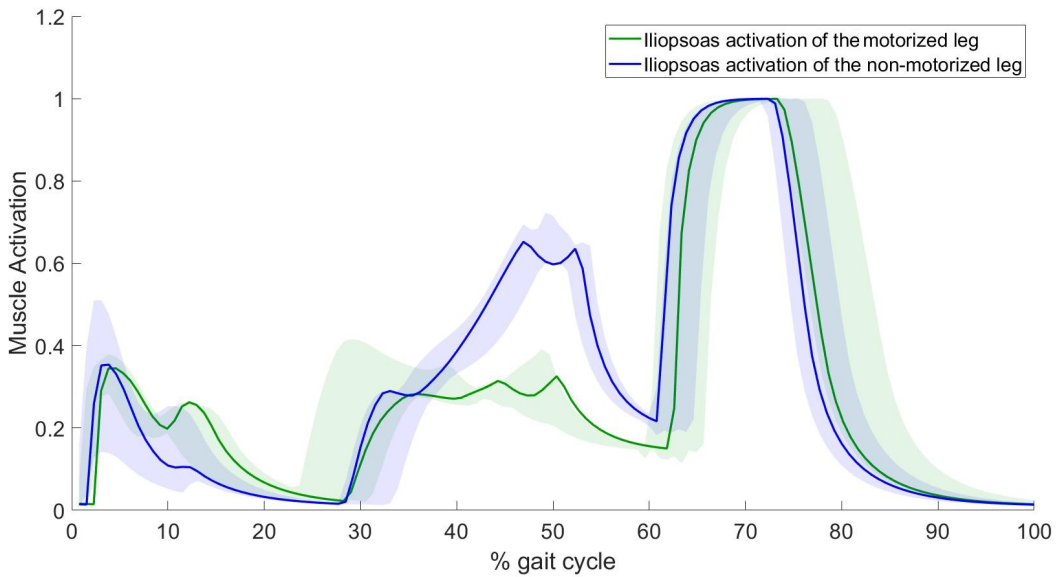


Figure 5.6: Comparison between the activation signals of the iliopsoas muscles between the motorized and non-motorized legs when using the Alpha torque profile, where the shaded area is all the range of obtained values, while the solid line is the obtained one once the walking had stabilized.

As we can see in Figure 5.4 and in Figure 5.5, we have a notable difference, in matter of activation, for the hamstring muscles and the gluteus maximus muscles between the motorized and the non-motorized leg. Once the walking is stable, we can see in Figure 5.4, the maximum level of activation needed during the gait cycle for the motorized leg, is practically half that of the non-motorized one, for the hamstrings muscle. For the gluteus maximus muscle, the difference is not so extreme, but the difference in terms of activation is also noticeable.

The iliopsoas muscle is the only muscle which does not present major differences between the motorized and non-motorized legs, as we can see in Figure 5.6. In fact, at this point in our research period, we had not found a single case where the iliopsoas presented a remarkable difference between both legs in regard to activation

The Alpha torque profile seems like a candidate worth trying for the experiments, but not without forgetting that a user with low muscular force at the iliopsoas muscle would not be suitable to use the presented torque profile, since at some point in the gait, we are mostly demanding the same amount of power for the afflicted leg as for the healthy one.

5.2.2 Experiment Evaluation

Now we will follow with the analysis of the actual experiment, starting with the comparison between the theoretical torque profile and the one exerted by the motors as depicted in Figure 5.7:

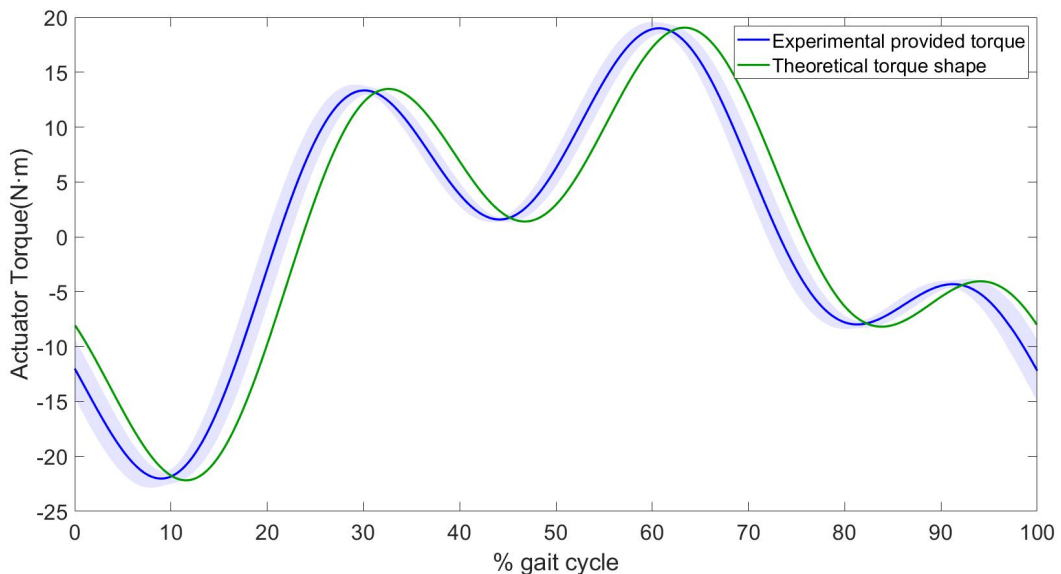


Figure 5.7: Comparison between the theoretical Alpha torque profile and the one received by the actuators, where the solid line is the mean between all the obtained values and the shaded area is the standard deviation.

As we can see in Figure 5.7, the torque is slightly shifted. Since the shifting is so small, the user should not be able to feel a major discomfort from the lack of synchronization.

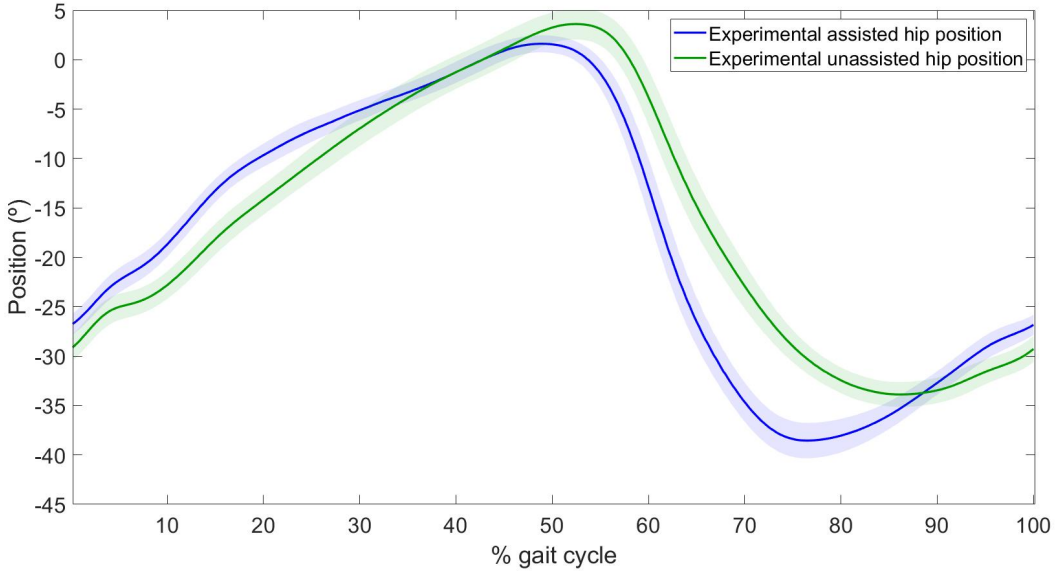


Figure 5.8: Comparison between the hip position of the user when no assistance is received and when the Alpha torque profile is being applied on the actuators, where the solid line is the mean between all the obtained values and the shaded area is the standard deviation.

It would be natural that a healthy user receiving assistance would have larger peak angle, but in our case, we can see in Figure 5.8 that the peak angle is decreased when assistance is received while the valley is increased (talking in absolute values), meaning that we can suspect that the assistance is indeed not synchronized with the user's natural walking gait. We can check this by looking at Figure 5.9 for a graphical comparison:

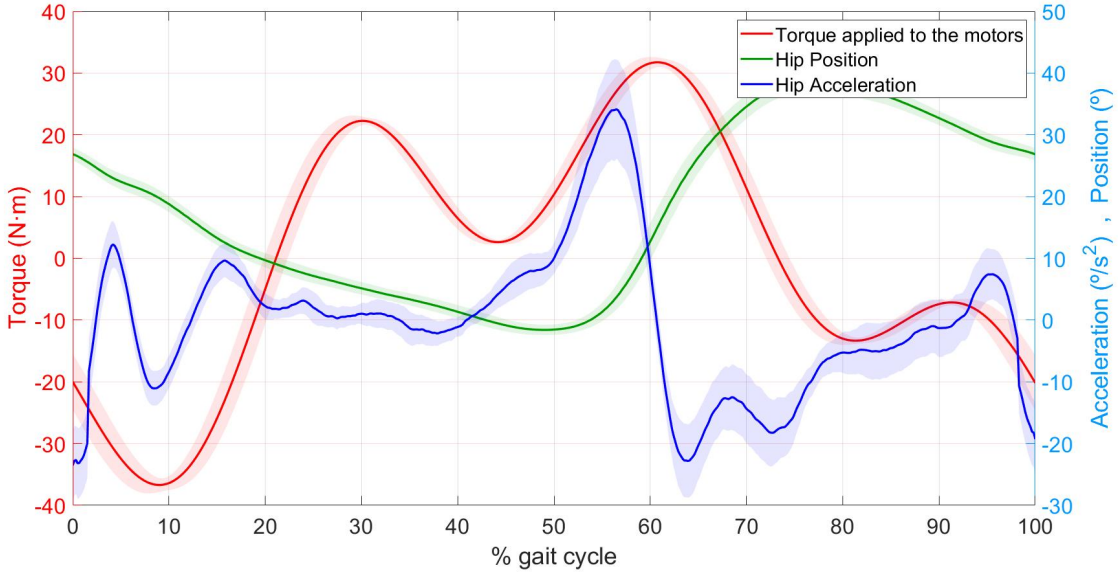


Figure 5.9: Display of the torque applied to the hip, the hip position and the hip acceleration, where a solid line is the mean between all the obtained values and a shaded area is the standard deviation.

We have to take into consideration that the encoders integrated in the orthosis actuators were used to measure the hip position. Therefore, the velocity could be found integrating the position measurement, and in the same way, we could find the acceleration by integrating the

velocity.

Take into account that using this kind of approach has the drawback of yielding noisy results due to integration error. Because of this, even though the signal has been filtered, the values for the acceleration might be noisy, and are not fully reliable.

Looking at the graphs we cannot know without further study if a performed motion was desired or if it was governed by the orthosis, but we can easily see cases where the torque and the acceleration do not match. For example at 30% of the gait cycle, we have a torque overshoot, but instead we do not experience a consequent acceleration. This means that for this particular moment the robot is providing a torque which is fighting against the user instead of aiding him/her.

A certain degree of divergence is tolerated between the torque and the acceleration, but we can clearly see, between 60% and 70% of the gait cycle, that the torque is not only positive, but also at its highest value, while the acceleration is negative instead. At this particular moment, which we can observe from the position graph that is in the middle of the swing state, the user was feeling torque in one direction while he/she was pushing in the opposite.

In sum, looking at this data, we can easily see that while wearing the orthosis the user was not experiencing a convenient assistance.

User Reviews

The set of all users' opinions and reactions regarding the orthosis experience included the feeling that the orthosis was providing assistance, meaning that the provided torque was synchronous with the user (at least to a certain degree), but that it was too strong, that the walking felt completely unnatural and was not comfortable anymore. They also reported that they lost the feeling of being able to control their own walking, since now the orthosis was forcing the user to perform unnatural motions. Thus, we could conclude that the provided torque profile was indeed aiding the user at the cost of making him/her uncomfortable with the resulting walking gait.

5.3 Beta experiment

The second experiment was to use the first torque profile obtained through the simulator that presented less energy consumption for the iliopsoas muscle of the motorized leg than for the non-motorized one.

5.3.1 Simulation evaluation

As a matter of practicality, to avoid confusion, we will refer to this experiment as the Beta experiment. And as with the previous experiment, we will refer to the provided torque profile of this one as the Beta torque profile.

Here, in Figure 5.10, we can see its shape obtained using the optimizer:

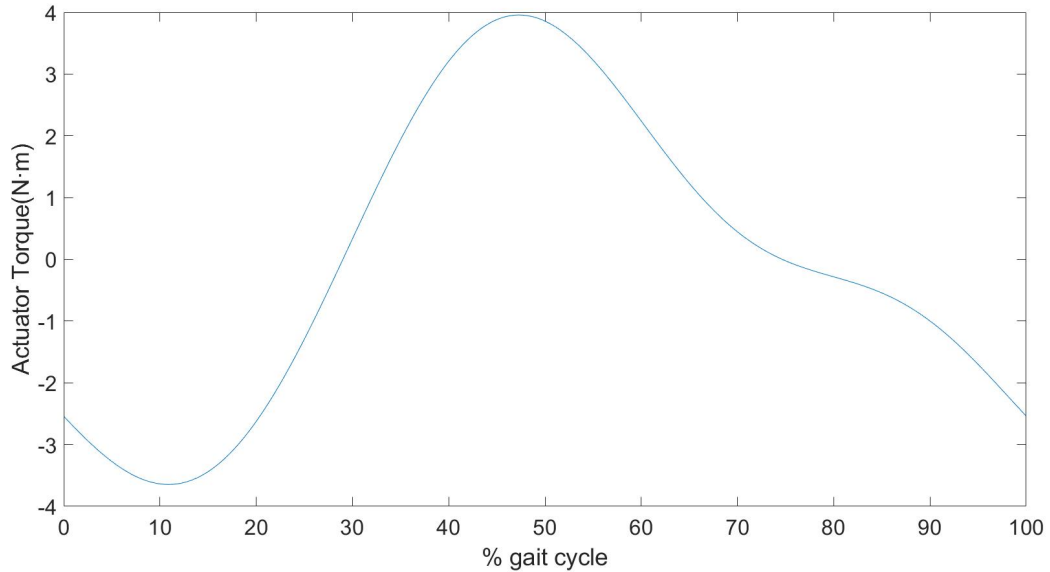


Figure 5.10: Shape of the Beta torque profile, obtained using the simulator.

Following the same procedure as with experiment Alpha, we will provide the comparison graphs of the activation signals received by the muscle groups between the motorized and the non-motorized legs, obtained during simulations:

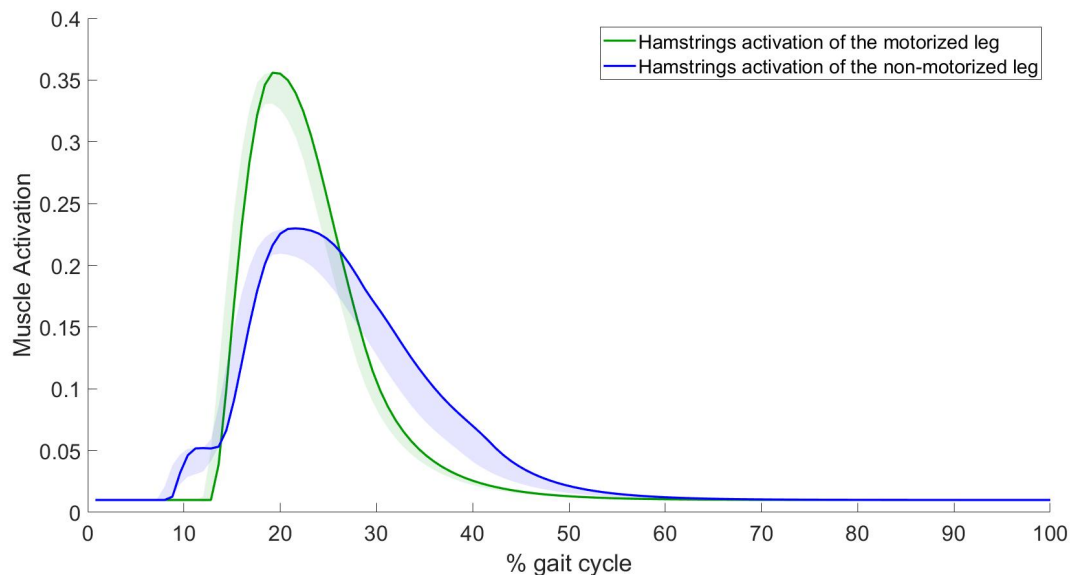


Figure 5.11: Comparison between the activation signals of the hamstring muscles between the motorized and non-motorized legs when using the Beta torque profile, where the shaded area is all the range of obtained values, while the solid line is the obtained one once the walking had stabilized.

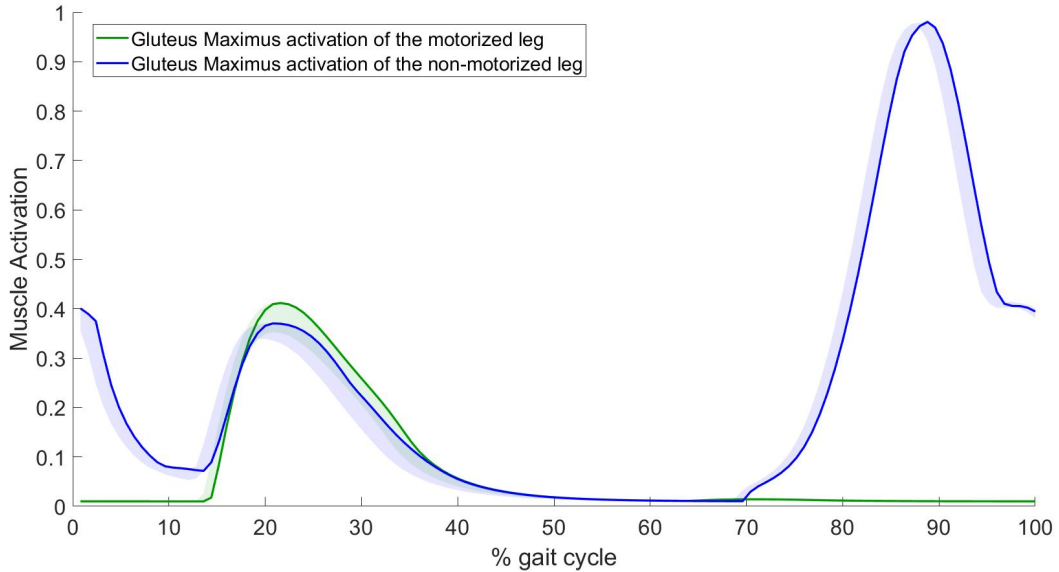


Figure 5.12: Comparison between the activation signals of the gluteus maximus muscles between the motorized and non-motorized legs when using the Beta torque profile, where the shaded area is all the range of obtained values, while the solid line is the obtained one once the walking had stabilized.

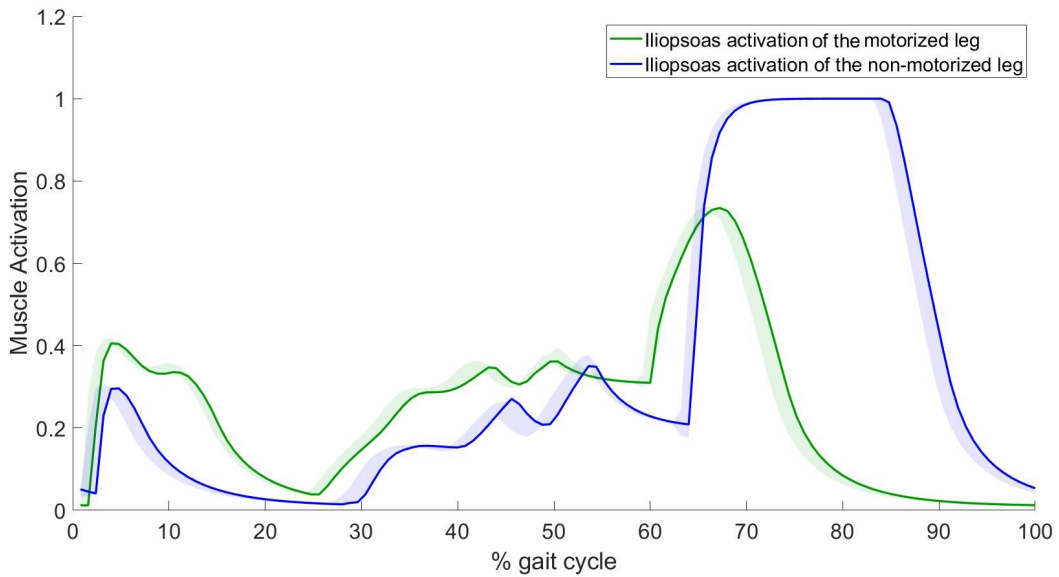


Figure 5.13: Comparison between the activation signals of the iliopsoas muscles between the motorized and non-motorized legs when using the Beta torque profile, where the shaded area is all the range of obtained values, while the solid line is the obtained one once the walking had stabilized.

As we can see in Figure 5.11, Figure 5.12 and Figure 5.13, for all 3 muscles a notable difference is presented, in terms of activation, between the motorized and the non-motorized leg. Once the stable gait has been reached, we can clearly see that the activation for all of them is lower for the motorized leg than for the non-motorized one.

In Figure 5.11 we can see that for the hamstring muscles, the assisted leg requires more activation than the healthy one but is still at an activation level of 0.35, low enough to consider

it acceptable. The shapes are similar but with a change in its amplitude. When we use the Beta torque profile, we can see in Figure 5.12 that for the gluteus maximus muscle, in fact, the activation is lower for the motorized leg, at a cost of having an overshoot on the non-motorized one. This case is interesting because we have achieved a good energy reduction for the injured leg at the cost of making the healthy leg work more. As we can see, this overshoot was not present in the healthy activation graphs from the Figure 3.5 in section 3.1.1 [Healthy gait simulation](#), and we can affirm that this torque profile would work for a user with one healthy leg and one with low strength, but it would not for a user with two weak legs.

Finally, in Figure 5.13, the iliopsoas profile displays a considerable reduction in the activation between the motorized and the non-motorized legs, making it the only case found using the optimizer where the iliopsoas did not need to use 100% of its activation at a given point. This is a very important and interesting case, because according to [39] the iliopsoas is the muscle that consumes the most energy during the walking cycle, and more precisely, during the hip flexion-extension motion. In light of this, it has been a compelling point to find a case where the received assistance could notably release some stress on this muscle.

In view of these findings, the Beta torque profile seems to be a promising candidate for the experiments with much potential due to its singular properties, but again, taking into account, that we might be assisting the iliopsoas muscle of the feeble leg at the cost of increasing reliance on the gluteus maximus muscle to a point where typical walking would not normally reach.

5.3.2 Experiment evaluation

In this sub-section, starting with Figure 5.14, by comparing the theoretical torque profile and real the one exerted by the motors, we will perform the analysis of the actual experiment:

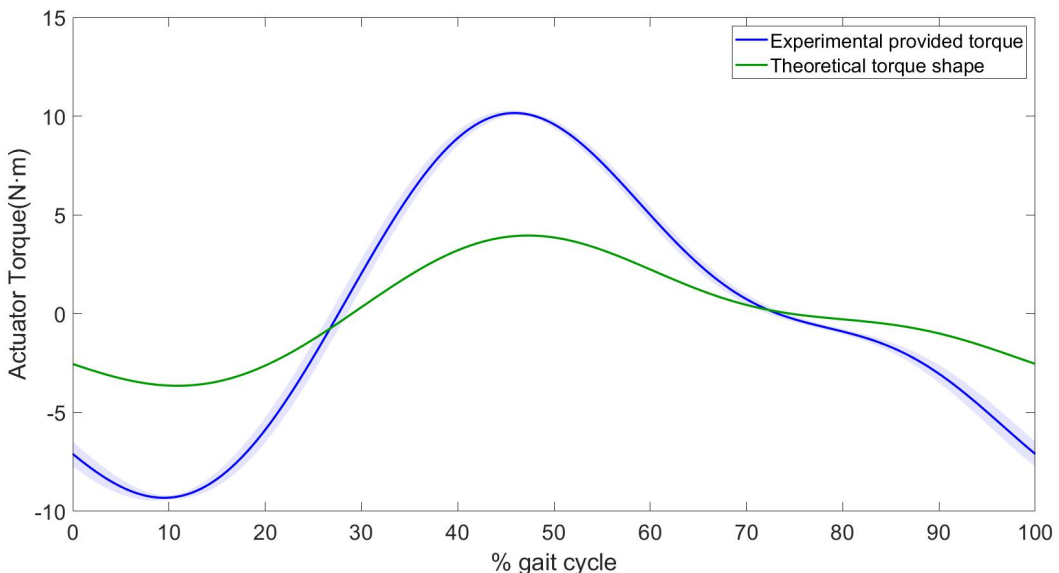


Figure 5.14: Comparison between the theoretical Beta torque profile and the one received by the actuators, where the solid line is the mean between all the obtained values and the shaded area is the standard deviation.

As we can see, the wave is slightly shifted, as happened also with the Alpha experiment. However, the most notable difference is the difference between the amplitudes. This difference

is because the user was walking at a faster rate than the original rate used during simulations, as we explained at the beginning of this chapter.

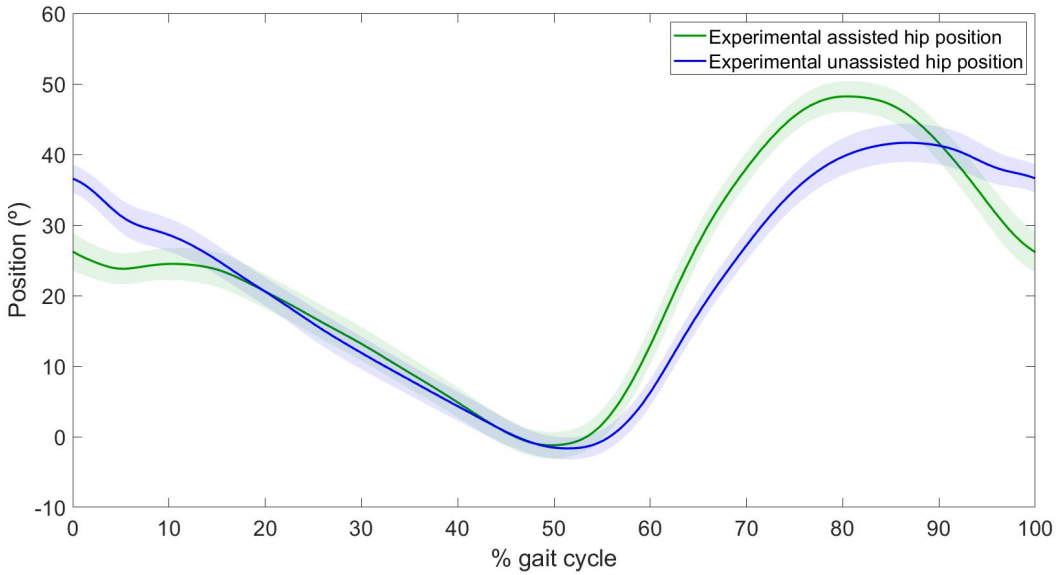


Figure 5.15: Comparison between the hip position of the user when no assistance is received and when the Beta torque profile is being applied on the actuators, where the solid line is the mean between all the obtained values and the shaded area is the standard deviation.

We can see in Figure 5.15 that a large percentage of the gait cycle is equal or very similar in the assisted and non-assisted cases, but we can see that the swing ends prematurely at approximately 50° instead of the original 40° when no assistance was received. This means that the user is taking smaller steps, probably because the orthosis is forcing the user to finish the swing earlier. We can check this by looking at the following Figure 5.16:

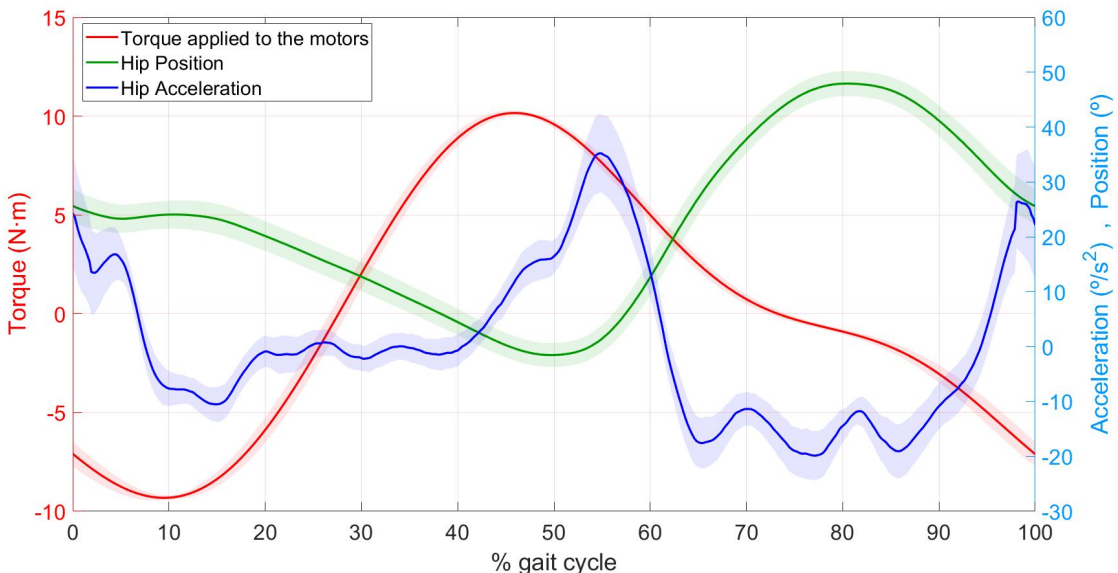


Figure 5.16: Display of the torque applied to the hip, the hip position and the hip acceleration, where a solid line is the mean between all the obtained values and a shaded area is the standard deviation.

We can see that compared with experiment Alpha, the synchronization between the torque

and the acceleration is much more notable. For example, during the swing, the switch between positive and negative acceleration is not happening during the torque peak, instead it happens when the torque is getting close to switch sign too. We can see, however, that at the end of the gait cycle, we have a positive acceleration overshoot, which does not match the direction of the torque. This might be the cause of the step being shorter than in the non-motorized case, but again, the variation in the hip position is very small.

Analytically talking, this torque profile proves to be more synchronized than the one seen in the Alpha experiment, and the user should not feel major discomforts when testing it.

User Reviews

The set of all users' opinions and reactions regarding the orthosis experience included reports that the assistance received felt really comfortable. They said that their walking was not altered by the orthosis in any bothersome way, that the assistance felt in good synchronization during all the gait cycle. The only negative comment was that at the end of the swing, before the user could get ready for the heel-strike, the torque was opposing the desired movement in order to the end of the swing.

Thus we can see that the analytical results matched the users' thoughts, regarding the unexpected torque at the end of the swing. Nonetheless, we have verified in a subjective way that the users do feel comfort with the Beta torque profile, concluding that the assistance achieved with this torque profile was a success.

CHAPTER 6

Conclusions and Further Work

The aim of this project was to find a successful control strategy for the eWalk orthosis using a neuro-mechanical model based on reflex controllers to run the simulations. To do so, we started by extracting what we called, the biological torque profile of a healthy gait directly from the Geyer's model[41]. Our first attempt was to use this torque profile as an input for the SCONE optimizer in order to find the most optimal torque profile possible as an input for the motors of a real orthosis. We have modeled the torque profile into a mathematical function, and we have proven that the method chosen for this task seriously changes the optimization result. Using a polynomial function resulted in obtaining discontinuities in the optimized torque profile, due to the drastic changes in its shape when we modify, even slightly, the variables of the polynomial. Because of this, this approach was rapidly discarded, but we have to take into consideration that polynomial functions require a low amount of variables to determine their shape. Therefore, a good approach for further investigation would be to implement a criterion which forced the found polynomial to start and finish at the same point, getting rid of any potential discontinuities. Instead, using a Fourier series approximation of the torque profile has proven to yield outstanding results due to its periodic properties, at the cost of requiring more variables, therefore, consuming more time to optimize it.

However, to use the Fourier series approach, we have implemented a method to chain different sets of waves, with unknown starts or endings. This method has proven to be not only very useful, but also very robust. It not only chains the current wave with the upcoming one, but it also tries to predict the period of this second one. During both simulations and experiments, this method has proven to be reliable since it could rapidly converge and synchronize with the user's walking speed. However, knowing that the only input for this kind of control is the time between steps, it has demonstrated better results when the walking speed is faster, i.e. when we detect heel-strikes at a higher rate.

We have shown two methods for detecting heel-strokes, compatible with the sensors of the eWalk robot, the first one relying on the encoders of the eWalk actuators and the second one relying on using force sensors on the user's shoes. This second method has proven to have a low level of reliability because it has been shown that in some cases the kinematics of the hip have the same values for a heel-strike as for a non-heel-strike. Also we have to take into consideration that, as seen in section [1.2.1 Gait kinematics and dynamics](#), the speed and position of the hip relies on the user's speed, and stature, making the kinematics even more inconstant. It has to be said, though, that it has the advantage of not needing any additional sensors than the ones integrated in the motors themselves. That being said, if further investigation requires this approach, it would be recommendable to use the readings from both legs jointly, instead of considering the readings from each leg as an independent entity. Doing so would double the amount of available variables that we could use in such task.

Resuming with the torque profiles, the biological torques obtained from Geyer's model were discarded because we could not find any satisfactory result through optimization. This can be due to the fact that the obtained torque profile presented too many optimization variables (using the Fourier series approximation), therefore it took more time to run each optimization, making it hard to find a reasonable torque profile within the established duration of this research internship. That does not mean this approach would not work. As has been said during the project, the neuro-mechanical model based on reflex controllers has displayed a great capacity for obtaining good quality gaits, therefore, we believe that from the biological torque extracted from it, there still might be some valid torque profiles that we have not explored.

Since the biological torque obtained from Geyer's model has been discontinued, using the torque profile from [20] as a starting point for the SCONE optimizer has proven to be a success. Its shape could be modeled into a Fourier series function using fewer variables, therefore, obtaining promising torque profiles through optimization has proven to be faster.

To determine if a torque profile found by optimizing the torque profile from [20] was promising, as [20] suggested, we used the activation signals of our desired muscles, in our case, the iliopsoas, the hamstrings and the gluteus maximus.

We have run several optimizations using the Geyer model and it has turned out to be more robust than anticipated. We could observe that we could find many potential solutions, where the model was capable of obtaining very good gaits against unfavourable torque profiles, also taking into account that we were providing asymmetrical assistance (motorizing just one leg).

In section 4.3 The SCONE cost functions, we have presented several cost functions, which have proven very useful for the SCONE optimizer by helping it find better torque profiles, highly decreasing the needed amount of time. Taking into account that the model was asymmetrical, the most relevant cost function was the last one, which forced a lower activation for the motorized leg than for the non-motorized one.

We encourage any further investigation in this field to consider the following advice: Trying to implement an asymmetrical assistance has proven to be time consuming. Even though our reasons for taking this approach were justified, it was harder for the simulator to find a reasonable result. Therefore, trying to implement the same assistance in both legs and simply checking if the robot has less energy consumption between a case with assistance in both legs and a case without assistance would be a faster method for running simulations. Another valid approach would be to weaken the robustness of the model, given that it is capable to obtain a good walking gait that even with problematic torques. This could be done by weakening a particular muscle and trying to find valid torque profiles from this point of departure. Using this method, the simulator would discard any option that would not be aiding the weakened muscle and, therefore, obtain results in a faster way.

We have tested the promising torque profiles with real subjects in order to seek verification. Three kinds of analyses have been run. The first one was to check the difference between the applied torque profile and the one real one exerted by the orthosis actuators. The second one was a comparison between the hip position of the user while walking with assistance and without it. The third one was to check that the assisting torque was in synchronization with the hip angular acceleration. This third one has proven to be the one which we can extract the most information from, since it was simple to see at which moments in the gait cycle the torque was

not going in the same direction as the acceleration, meaning that the actuators' assistance was fighting against the user.

We have to take into consideration that we did not possess as much measurement equipment as we would have liked, and therefore, much feedback on our experiments came from the subjective opinion received from the users. The users who tested our particular torque profiles reported feeling assistance for both of them, but a high level of discomfort for the first one. The observations reported by the users matched the conclusions found during analysis, proving that the three analysis methods presented are correct.

Nevertheless, in further research, it would be highly recommendable to use oxygen consumption sensors in order to obtain an empirical reading of the users' level of fatigue, and thereby know if there is an actual decrease in the users' energy consumption while receiving assistance. It would also provide a great deal of feedback to use EMG sensors, so we could also compare the activation measurements obtained through simulation and real measurements obtained during experiments with humans.

Bibliography

- [1] D. H. Paterson, D. Govindasamy, M. Vidmar, D. A. Cunningham, and J. J. Koval, "Longitudinal study of determinants of dependence in an elderly population," *Journal of the American Geriatrics Society*, vol. 52, no. 10, pp. 1632–1638, Oct 2004.
- [2] J. E. Cohen, "Human Population: The Next Half Century," pp. 1172–1175, Nov 2003.
- [3] E. C. Jansen, D. Vittas, S. Hellberg, and J. Hansen, "Normal gait of Young and old men and women: Ground reaction force measurement on a treadmill," *Acta Orthopaedica*, vol. 53, no. 2, pp. 193–196, 1982. [Online]. Available: <https://www.tandfonline.com/action/journalInformation?journalCode=ior20>
- [4] J. H. Sheldon, "The effect of age on the control of sway," *Gerontologia clinica*, vol. 5, pp. 129–138, 1963. [Online]. Available: <https://pubmed.ncbi.nlm.nih.gov/13977074/>
- [5] L. A. Brown, A. Shumway-Cook, and M. H. Woollacott, "Attentional demands and postural recovery: The effects of aging," *Journals of Gerontology - Series A Biological Sciences and Medical Sciences*, vol. 54, no. 4, 1999. [Online]. Available: <https://pubmed.ncbi.nlm.nih.gov/10219006/>
- [6] R. Baud, A. Ortlib, J. Olivier, M. Bouri, and H. Bleuler, "HIBSO hip exoskeleton: Toward a wearable and autonomous design," in *Mechanisms and Machine Science*, vol. 48. Springer Netherlands, 2018, pp. 185–195. [Online]. Available: http://link.springer.com/10.1007/978-3-319-59972-4_14
- [7] J. Olivier, "Development of Walk Assistive Orthoses for Elderly EPFL," Ph.D. dissertation, 2016. [Online]. Available: <https://infoscience.epfl.ch/record/217937>
- [8] J. Olivier, A. Ortlib, M. Bouri, and H. Bleuler, "Mechanisms for actuated assistive hip orthoses," in *Robotics and Autonomous Systems*, vol. 73. Elsevier, Nov 2015, pp. 59–67.
- [9] H. Herr, "Exoskeletons and orthoses: Classification, design challenges and future directions," *Journal of NeuroEngineering and Rehabilitation*, vol. 6, no. 1, p. 21, Dec 2009. [Online]. Available: <https://jneuroengrehab.biomedcentral.com/articles/10.1186/1743-0003-6-21>
- [10] F. C. Anderson and M. G. Pandy, "Dynamic optimization of human walking," *Journal of Biomechanical Engineering*, vol. 123, no. 5, pp. 381–390, 2001. [Online]. Available: <https://pubmed.ncbi.nlm.nih.gov/11601721/>
- [11] T. Poluyi, "Control System Development for Six Degree of Freedom Spine Simulator," no. August 2014, 2014. [Online]. Available: https://www.researchgate.net/publication/270340667_Control_System_Development_for_Six_Degree_of_Freedom_Spine_Simulator

- [12] C. Schmitt and R. D. Clavel, “Orthèses fonctionnelles à cinématique parallèle et sérielle pour la rééducation des membres inférieurs,” Tech. Rep., 2007. [Online]. Available: <https://infoscience.epfl.ch/record/101059>
- [13] I. P. Pappas, M. R. Popovic, T. Keller, V. Dietz, and M. Morari, “A reliable gait phase detection system,” *IEEE Transactions on Neural Systems and Rehabilitation Engineering*, vol. 9, no. 2, pp. 113–125, 2001.
- [14] S. Mihecin, S. Ciklacakdir, M. Kocak, and A. Tosun, “Wearable motion capture system evaluation for biomechanical studies for hip joints,” *Journal of Biomechanical Engineering*, vol. 143, no. 4, apr 2021.
- [15] A. Roaas and G. B. Andersson, “Normal range of motion of the hip, knee and ankle joints in Male subjects, 30-40 years of age,” *Acta Orthopaedica*, vol. 53, no. 2, pp. 205–208, 1982. [Online]. Available: <https://pubmed.ncbi.nlm.nih.gov/7136564/>
- [16] C. BenAbdelkader, R. G. Cutler, and L. S. Davis, “Gait recognition using image self-similarity,” *Eurasip Journal on Applied Signal Processing*, vol. 2004, no. 4, pp. 572–585, apr 2004. [Online]. Available: <https://asp-eurasipjournals.springeropen.com/articles/10.1155/S1110865704309236>
- [17] M. W. Whittle, “Clinical gait analysis: A review,” *Human Movement Science*, vol. 15, no. 3, pp. 369–387, 1996.
- [18] G. Johansson, “Visual perception of biological motion and a model for its analysis,” *Perception Psychophysics*, vol. 14, no. 2, pp. 201–211, Jun 1973. [Online]. Available: <https://link.springer.com/article/10.3758/BF03212378>
- [19] P. M. Mills, S. Morrison, D. G. Lloyd, and R. S. Barrett, “Repeatability of 3D gait kinematics obtained from an electromagnetic tracking system during treadmill locomotion,” *Journal of Biomechanics*, vol. 40, no. 7, pp. 1504–1511, 2007. [Online]. Available: <https://pubmed.ncbi.nlm.nih.gov/16919639/>
- [20] M. H. Schwartz, A. Rozumalski, and J. P. Trost, “The effect of walking speed on the gait of typically developing children,” *Journal of Biomechanics*, vol. 41, no. 8, pp. 1639–1650, 2008. [Online]. Available: <https://pubmed.ncbi.nlm.nih.gov/18466909/>
- [21] C. L. Vaughan, B. L. Davis, and J. C. O’Connor, “Dynamics of human gait 2nd Edition,” Tech. Rep., 1999. [Online]. Available: <http://www.kiboho.co.za/GaitCD>
- [22] J. Duysens and H. W. Van De Crommert, “Neural control of locomotion; Part 1: The central pattern generator from cats to humans,” pp. 131–141, Mar 1998. [Online]. Available: <https://pubmed.ncbi.nlm.nih.gov/10200383/>
- [23] H. W. Van De Crommert, T. Mulder, and J. Duysens, “Neural control of locomotion: Sensory control of the central pattern generator and its relation to treadmill training,” *Gait and Posture*, vol. 7, no. 3, pp. 251–263, May 1998. [Online]. Available: <https://pubmed.ncbi.nlm.nih.gov/10200392/>
- [24] D. J. Farris, J. L. Hicks, S. L. Delp, and G. S. Sawicki, “Musculoskeletal modelling deconstructs the paradoxical effects of elastic ankle exoskeletons on plantar-flexor mechanics and energetics during hopping,” *Journal of Experimental Biology*, vol. 217, no. 22, pp. 4018–4028, Nov 2014.

- [25] G. S. Sawicki and N. S. Khan, "A Simple Model to Estimate Plantarflexor Muscle-Tendon Mechanics and Energetics During Walking With Elastic Ankle Exoskeletons," *IEEE Transactions on Biomedical Engineering*, vol. 63, no. 5, pp. 914–923, May 2016.
- [26] J. Markowitz and H. Herr, "Human Leg Model Predicts Muscle Forces, States, and Energetics during Walking," *PLOS Computational Biology*, vol. 12, no. 5, p. e1004912, May 2016. [Online]. Available: <https://dx.plos.org/10.1371/journal.pcbi.1004912>
- [27] C. Meijneke, G. Van Oort, V. Sluiter, E. Van Asseldonk, N. L. Tagliamonte, F. Tamburella, I. Pisotta, M. Masciullo, M. Arquilla, M. Molinari, A. R. Wu, F. Dzeladini, A. J. Ijspeert, and H. Van Der Kooij, "Symbitron Exoskeleton: Design, Control, and Evaluation of a Modular Exoskeleton for Incomplete and Complete Spinal Cord Injured Individuals," *IEEE TRANSACTIONS ON NEURAL SYSTEMS AND REHABILITATION ENGINEERING*, vol. 29, p. 2021. [Online]. Available: <https://doi.org/10.1109/TNSRE.2021.3049960>,
- [28] R. H. Miller, "A comparison of muscle energy models for simulating human walking in three dimensions," *Journal of Biomechanics*, vol. 47, no. 6, pp. 1373–1381, apr 2014.
- [29] T. L. Hill, "Theoretical formalism for the sliding filament model of contraction of striated muscle part II," pp. 105–159, 1976. [Online]. Available: <https://pubmed.ncbi.nlm.nih.gov/1135417/>
- [30] R. H. Miller, "Hill-Based Muscle Modeling," in *Handbook of Human Motion*. Springer International Publishing, 2018, pp. 1–22. [Online]. Available: https://doi.org/10.1007/978-3-319-30808-1_203-2
- [31] B. R. Umberger and R. H. Miller, "Optimal Control Modeling of Human Movement," in *Handbook of Human Motion*. Springer International Publishing, 2017, pp. 1–22. [Online]. Available: https://link.springer.com/referenceworkentry/10.1007/978-3-319-30808-1_177-1
- [32] T. Siebert, C. Rode, W. Herzog, O. Till, and R. Blickhan, "Nonlinearities make a difference: Comparison of two common Hill-type models with real muscle," *Biological Cybernetics*, vol. 98, no. 2, pp. 133–143, Feb 2008. [Online]. Available: <https://link.springer.com/article/10.1007/s00422-007-0197-6>
- [33] A. M. Gordon, A. F. Huxley, and F. J. Julian, "The variation in isometric tension with sarcomere length in vertebrate muscle fibres," *The Journal of Physiology*, vol. 184, no. 1, pp. 170–192, May 1966. [Online]. Available: [/pmc/articles/PMC1357553/?report=abstract](https://www.ncbi.nlm.nih.gov/pmc/articles/PMC1357553/?report=abstract)<https://www.ncbi.nlm.nih.gov/pmc/articles/PMC1357553/>
- [34] Y. Z. Arslan, D. Karabulut, F. Ortes, and M. B. Popovic, "Exoskeletons, Exomusculatures, Exosuits: Dynamic Modeling and Simulation," in *Biomechatronics*. Elsevier, Jan 2019, pp. 305–331.
- [35] M. Blümel, S. L. Hooper, C. Guschlbauer, W. E. White, and A. Büschges, "Determining all parameters necessary to build Hill-type muscle models from experiments on single muscles," *Biological Cybernetics*, vol. 106, no. 10, pp. 543–558, Nov 2012. [Online]. Available: <https://link.springer.com/article/10.1007/s00422-012-0531-5>
- [36] W. Herzog, "History dependence of skeletal muscle force production: Implications for movement control," *Human Movement Science*, vol. 23, no. 5, pp. 591–604, Nov 2004.

- [37] B. R. Umberger, K. G. Gerritsen, and P. E. Martin, “A model of human muscle energy expenditure.” *Computer methods in biomechanics and biomedical engineering*, vol. 6, no. 2, pp. 99–111, 2003. [Online]. Available: <https://www.tandfonline.com/action/journalInformation?journalCode=gcmb20>
- [38] D. S. Pamungkas, W. Caesarendra, S. Susanto, H. Soebakti, and R. Analia, “Overview: Types of lower limb exoskeletons,” Nov 2019.
- [39] C. L. Dembia, A. Silder, T. K. Uchida, J. L. Hicks, and S. L. Delp, “Simulating ideal assistive devices to reduce the metabolic cost of walking with heavy loads,” *PLoS ONE*, vol. 12, no. 7, Jul 2017. [Online]. Available: <https://pubmed.ncbi.nlm.nih.gov/28700630/>
- [40] T. Geijtenbeek, “SCONE: Open Source Software for Predictive Simulation of Biological Motion,” *Journal of Open Source Software*, vol. 4, no. 38, p. 1421, Jun 2019. [Online]. Available: <https://doi.org/10.21105/joss.01421>
- [41] H. Geyer and H. Herr, “A Muscle-reflex model that encodes principles of legged mechanics produces human walking dynamics and muscle activities,” *IEEE Transactions on Neural Systems and Rehabilitation Engineering*, vol. 18, no. 3, pp. 263–273, Jun 2010.
- [42] A. Seth, J. L. Hicks, T. K. Uchida, A. Habib, C. L. Dembia, J. J. Dunne, C. F. Ong, M. S. DeMers, A. Rajagopal, M. Millard, S. R. Hamner, E. M. Arnold, J. R. Yong, S. K. Lakshmikanth, M. A. Sherman, J. P. Ku, and S. L. Delp, “OpenSim: Simulating musculoskeletal dynamics and neuromuscular control to study human and animal movement,” *PLOS Computational Biology*, vol. 14, no. 7, p. e1006223, Jul 2018. [Online]. Available: <https://dx.plos.org/10.1371/journal.pcbi.1006223>
- [43] A. Kalinowska, T. A. Berrueta, A. Zoss, and T. Murphey, “Data-Driven Gait Segmentation for Walking Assistance in a Lower-Limb Assistive Device,” *Proceedings - IEEE International Conference on Robotics and Automation*, vol. 2019-May, pp. 1390–1396, Feb 2019. [Online]. Available: <http://arxiv.org/abs/1903.00036>
- [44] Y. Sun, J. S. Hare, and M. S. Nixon, “Detecting heel strikes for gait analysis through acceleration flow,” *IET Computer Vision*, vol. 12, no. 5, pp. 686–692, aug 2018. [Online]. Available: <https://onlinelibrary.wiley.com/doi/10.1049/iet-cvi.2017.0429>
- [45] D. Fitzpatrick, *Implantable electronic medical devices*, 2014. [Online]. Available: <https://www.elsevier.com/books/implantable-electronic-medical-devices/fitzpatrick/978-0-12-416556-4>
- [46] J. Ye, H. Wu, L. Wu, J. Long, Y. Zhang, G. Chen, C. Wang, X. Luo, Q. Hou, and Y. Xu, “An Adaptive Method for Gait Event Detection of Gait Rehabilitation Robots,” *Frontiers in Neurorobotics*, vol. 14, p. 38, Jul 2020. [Online]. Available: <https://www.frontiersin.org/article/10.3389/fnbot.2020.00038/full>
- [47] D. J. Higham and N. J. Higham, *MATLAB guide*. Siam, 2016, vol. 150.
- [48] Q. Wu, X. Wang, F. Du, and X. Zhang, “Design and control of a powered hip exoskeleton for walking assistance,” *International Journal of Advanced Robotic Systems*, vol. 12, no. 3, p. 18, Mar 2015. [Online]. Available: <http://journals.sagepub.com/doi/10.5772/59757>
- [49] Y. Tan, D. Lau, M. Liu, P. Bidaud, and V. Padois, “Minimization of the rate of change in torques during motion and force control under discontinuous constraints,” in *2015 IEEE International Conference on Robotics and Biomimetics, IEEE-ROBIO 2015*. Institute of Electrical and Electronics Engineers Inc., 2015, pp. 2621–2628.

- [50] M. A. Sherman, A. Seth, and S. L. Delp, “Simbody: Multibody dynamics for biomedical research,” in *Procedia IUTAM*, vol. 2. Elsevier B.V., Jan 2011, pp. 241–261.
- [51] H. Geyer, A. Seyfarth, and R. Blickhan, “Compliant leg behaviour explains basic dynamics of walking and running,” *Proceedings of the Royal Society B: Biological Sciences*, vol. 273, no. 1603, pp. 2861–2867, Nov 2006. [Online]. Available: <https://royalsocietypublishing.org/>
- [52] C. F. Ong, T. Geijtenbeek, J. L. Hicks, and S. L. Delp, “Predicting gait adaptations due to ankle plantarflexor muscle weakness and contracture using physics-based musculoskeletal simulations,” *PLoS computational biology*, vol. 15, no. 10, p. e1006993, Oct 2019. [Online]. Available: <https://doi.org/10.1371/journal.pcbi.1006993>
- [53] N. Hansen, “The CMA Evolution Strategy: A Comparing Review,” in *Towards a New Evolutionary Computation*. Springer Berlin Heidelberg, Jun 2007, pp. 75–102.
- [54] N. Hansen, “The CMA Evolution Strategy: A Tutorial,” apr 2016. [Online]. Available: <http://arxiv.org/abs/1604.00772>